Computational Fluid Dynamic and Oxygen Transport Model of the Human Cardiopulmonary System

Arianna Worthy[1], Grayson Hawkins[1], Kwai Wong[2]

[1] Tickle College of Engineering, University of Tennessee, Knoxville

[2] Ph.D., Research Assistant Professor, Tickle College of Engineering, University of Tennessee, Knoxville

1 Abstract

In this project, we create a representative model of the cardiopulmonary system with a focus on the bulk/intensive properties of the fluids involved. We first observe the geometry of the pulmonary system and its immediate capillaries before using Comsol 5.2a to conduct stationary and transient finite element method simulations using the Navier-Stokes equations for computational fluid dynamic analysis and the Maxwell-Stefan equations for oxygen transport analysis.Our results include test cases for the 1st-3rd bifurcations of the tracheobronchial tree with a lung/blood interface, a starting point for future researchers to continue work in bifurcating furthering into the chest cavity and simulating a variety of breathing conditions.

2 Introduction

Current studies on the state of computational science in the medical field point towards a future in which physicians have easy and open access to individualized models of a patient's pulmonary and major cardiovascular features. The wealth of publications on this subject begin with aerosol deposition studies using cast models of the lung (Proetz 1951), up to simulation and verification on modern systems and softwares (Kim & Fisher 1999; Longest et al. 2016) and experimental validation of the fluid flow in such models (Minard et al. 2012). More recently, publications have addressed computational science applications for pre-op, real-time, and post-op analysis (Pennati et al. 2013; Zhao K et. al 2014) including a study of particular note, the computational analysis of "the hydrodynamic performance, oxygen transfer, and blood damage potential [of an artificial pump-lung]." (Zhongjun J Wu et al. 2011). This particular field boasts well-established methods of obtaining an accurate 3D model of a patient's lungs down to the 3rd~5th bifurcation (Weidong Mi 2015), but where is the plug-and-play framework of equations and test

cases to properly apply finite element analysis to these models? This project aims to create a useable visual system that physicians, researchers, and the public can modify with various properties to get a detailed analysis how those properties will change based on external or internal variables.

This project was split into two distinct parts, and the organization of this paper reflects that. In section 3.1 we discuss the development of our pulmonary models and in section 3.2 and 3.3, we discuss the development of our hemodynamic and oxygen transport simulations. Likewise, results and discussions are split into these divisions.

3 Model Development

Our philosophy is that the basics of accomplishing any complex result in a CFD simulation are beginning with a simple geometry, benchmarking key variables (pressure, velocity, oxygen content), then revising parts of the model based on those results. We did not have access to 3D models of the human tracheobronchial tree, but the the focus of our research was to make a *representative* model of the pulmonary system and its immediate cardiovascular features that can be easily modified for various scenarios. After beginning our project in 3D, we quickly switched to 2D and continued in this manner for the rest of the time.

First we will list the relevant equations and known values for these systems.

Ideal Gas Law:
PV=nRT
For the initial conditions of inspiration and expiration, we are making the assumption that temperature inside the body and outside the body is the same, and we do not lose any mass.

Henry's Law:
$\frac{pO2}{KH}$ = concentration of O_2 in a solvent
Henry's Law allows us to know the amount of oxygen in our blood content. Knowing how much oxygen

Fick's Law:
$V = \frac{(\Delta P) \times A \times D}{t}$

In our simulation, we will use Fick's Law to calculate the rate at which oxygen is diffusing from the alveoli sac into pulmonary capillaries. This rate remains mostly constant for an idealized simulation, but can vary as alveoli sacs are lost.

The Alveolar Gas Equation:

$P_AO_2 = F_IO_2(P_{atm} - pH_2O)$

This particular equation yields the amount of oxygen that enters the the alveolar sac.

$P_aO_2 = \frac{paCO2}{RQ}$

Using the above equations tells us how much oxygen is leaving the alveolar sac and entering the pulmonary capillaries that will carry its content to the heart.

Conservation of Mass, Momentum:

$$\sum_{i=0}^{n} Q = 0$$

For Q = Flow Rate normal to boundary (m³/s)
Assuming constant density ρ
Assuming normal flow across boundary

$$\sum F_x = \sum(M_x * U_{out}) - \sum(M_x * U_{in})$$

For M_x mass flow rate in one direction
For U average flow velocity at boundary in one same direction as M_x

Body Temperature:
We are assuming that all interaction are isothermal or near-isothermal at 37°C.

Pressure Difference in the lungs:
The pressure inside the lungs is referred to as intra-alveolar pressure. This is the driving force that allows a person's lung to inflate or deflate dependent on conditions. During inspiration, the intra-alveolar pressure is slightly negative, and during expiration, the pressure slightly positive. We will be using the atmospheric pressure at sea level (760 mm Hg) for our reference point. The pressure difference will vary between ∓1-3 mmHg at the terminal units of the lungs according to the literature. This is different from our results (see: Pulmonary Simulations).

Blood Pressure, Heart Rate, Total Cardiac Output:
Blood pressure is expressed as $\frac{systolic}{diastolic}$ where *systolic* is the highest point of pressure during a heart's contraction and *diastolic* is the lowest point of pressure during a heart's rest.

The blood pressure we will be assuming for "at-rest" simulations is $\frac{120}{80} mmHg$.
The heart rate we will be assuming for "at-rest" simulations is 60 BPM.

Blood pressure follows a sine wave in the following form

$$F(t) = \frac{(systolic - diastolic)}{2} * cos(\frac{BPM}{60} * 2\pi * t) + (diastolic + \frac{(systolic - diastolic)}{2})$$

According to Heart Physiology: From Cell to Circulation (Lionel H. Opie) the normal rate of blood flow is 6-8 L/min (pg. 460) for a male and 4-6 L/min for a female. We will be using 5.5L/min.

Properties of Blood:

$\rho = 1060\ kg/m^3$

$\mu = (0.003 \sim 0.004)\ Pa \bullet s$

$Q = 7.5\ E-5\ m^3/s$

$V = 5.5\ L\ =\ 0.0055\ m^3$

For our simulations, we will be using a viscosity of 0.0035 Pa-s. We are using a baseline approximation that ~7% of a human's body weight is blood.

Air Composition:

Atmospheric pressure is 760 mmHg. The air we inhale is composed of 78% N_2 and 21% O_2 and 1% Argon and the exhaled air is composed of 78% N, 17% O_2, 4% CO_2 and 1% Argon. Since we are primarily concerned with the oxygen and carbon dioxide levels, we will assume all argon to be nitrogen, giving an inhaled composition of 79%/21%/0%.

This makes the inspired oxygen mass fraction close to 0.233, which we will be using for our simulations.

Vapor Pressure from the H_2O in Lungs:

Lungs naturally moisten inhaled air. The vapor pressure of water at 37°C is 47 mmHg. This means that as air travels down the bronchial tree, the composition of air becomes (via eqn 2.1.4)...

Alveolar Gas Composition: 556/157/0/47 mmHg of $N_2/O_2/CO_2/H_2O$
Expired Gas Composition: 556/128/29/47 mmHg of $N_2/O_2/CO_2/H_2O$

Gas Exchange with The Blood:

The most important function the pulmonary system performs is exchanging oxygen and carbon dioxide to be stored and expired, respectively. This exchange happens simultaneously in alveolar sacs. The alveolar sacs diffuse the oxygen from the Alveolar Sacs into the pulmonary capillaries, and the sacs absorb carbon dioxide to be exhaled. The rate at which this takes place is dependent on a diffusion coefficient that varies based on the solubility of the diffusive fluid.

Once the oxygen is diffused into the blood, the oxygen begins to bind to Hemoglobin molecules (Hb) to form Oxygenated Hemoglobin (Hb_{O2}). This reaction follows the following stoichiometry:

$$Hb + 4O_2 \leftrightarrow Hb_{O2}$$
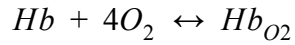
This reaction lowers the concentration of oxygen in the blood, this allows blood to hold *much* more oxygen as opposed to simply dissolving in blood.

3.1 Pulmonary System Development

3D Pulmonary Geometry

Our first simulation was done in 3D assuming a laminar flow (see Figure 1). It represents the trachea and the right/left mainstem bronchi. The 1st generation of the tracheobronchial tree was created using the cylinder tool and the dimensions of the geometry are specified in Table 1. Due to our limited CAD abilities, a cone was inserted to smooth the sharp corners of the bifurcation at the carina. The geometry is a *very* idealized representation of the pulmonary system. In a real system, the mainstem bronchi are not symmetrical and the bifurcation is much smoother. This test case was our first, rough step in the project and gave us proper benchmarks to move forward using a 2D geometry.
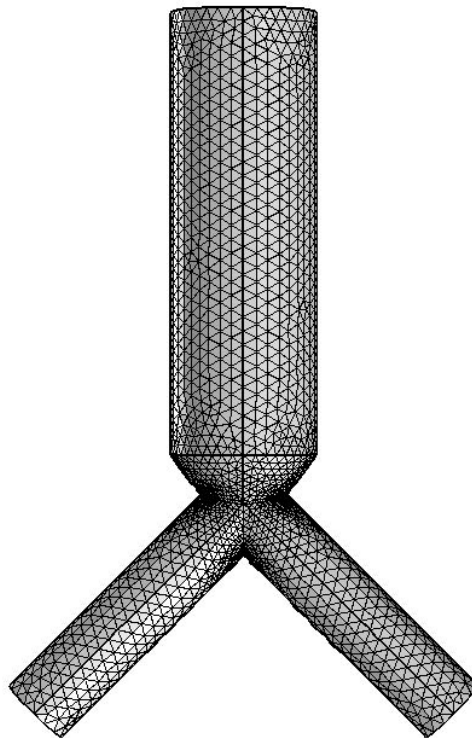
Figure 1

3D 1st Bifurcation Model	Radius (cm)	Length (cm)

Trachea	1.5	9
Right Mainstem Bronchus	0.75	6
Left Mainstem Bronchus	0.75	6
Cone (smoothing purpose)	1.5 (top) 0.75 (bottom)	1

Table 1

2D Pulmonary Geometries

By moving forward in 2 dimensions, we were able to create more precise geometries not readily available to us in 3D. Assuming the bronchi are all circular ducts, the parameterized length we are using is…

$$L_p(r) = \pi * r \text{ or } L_p(dia) = \tfrac{1}{4} * \pi * dia$$

For example, to find volumetric flow rate through an inlet of diameter d with an average velocity V…

$$Q = V * d * L_p(d) = V * \tfrac{1}{4} * \pi * d^2$$

The measurements for the first 2D geometry (Figure 3) were taken from a 2015 study from Weidong Mi et al. in which a sample of 2017 male and female participants from the Chinese population were measured for various tracheobronchial measurements. This study gave clinical measurements for the right and left main stem bronchi (RMS/LMS), and the right upper lobar bronchus. Due to lack of clinical data, we assigned the diameter of the left upper lobar bronchus based on the right upper lobar bronchus using the same ratio of LMS/RMS diameter.
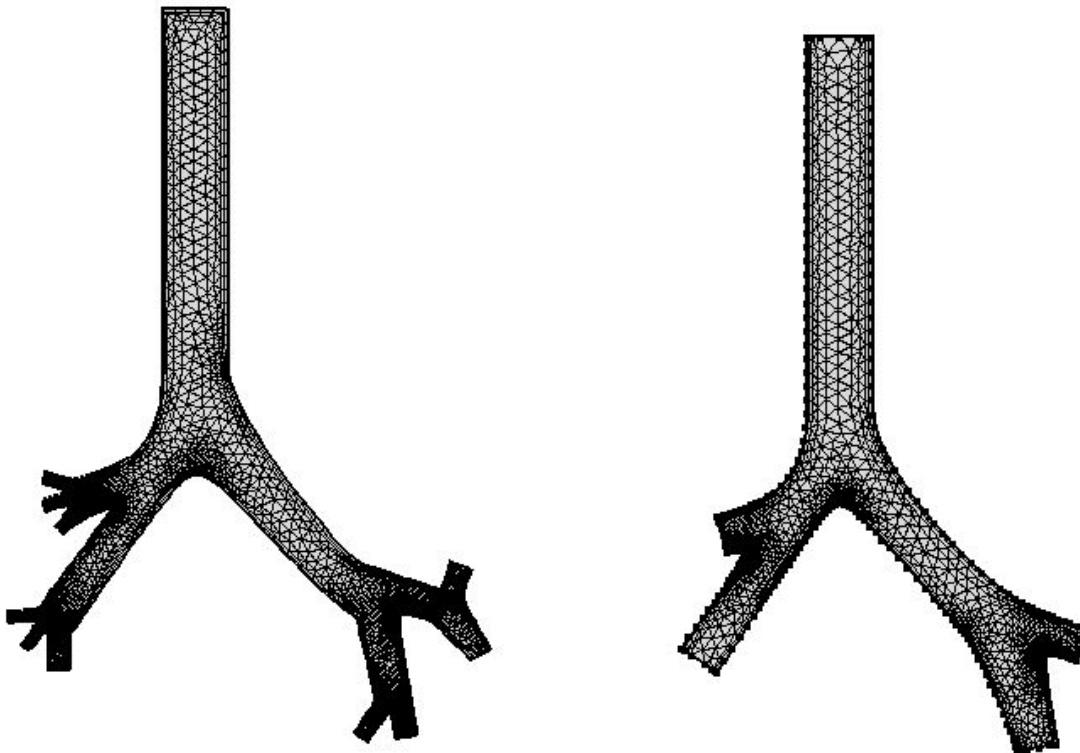
The second 2D pulmonary geometry (Figure 4) represents a continuation onto the third bifurcation of the lungs. It branches out to distinguish the upper lobe from the middle and lower lobe, showing several subsegmental bronchi.

Flow Rates for Pulmonary Simulation

Our pulmonary simulations were based on a tidal volume of 0.5L at 15 breaths per minute. These values are described as "at rest" breathing conditions by multiple textbook sources (Hlastala and Berger 2001; Des Jardins 2002). There are differences between inspiration and expiration when plotted on a volume-flow graph meaning that an inhale is a much smoother, constant flow while an exhale begins sharply at its max flow rate while linearly tapering off as flow becomes independent of effort (Hlastala and Berger 2001, pg. 55). To model this accurately, we modified outlet conditions using periodic waveform functions and a switch function between inspiration and expiration.
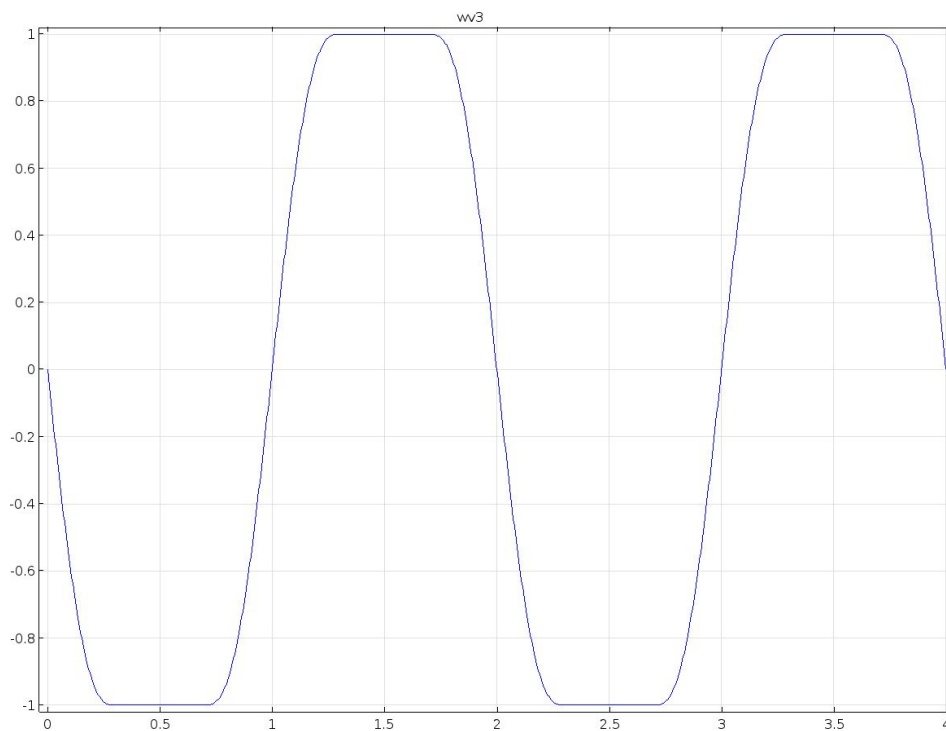
Figure 4

Figure 4 shows the inhale waveform graph that was used in all 2D transient simulations. The inhale waveform the following settings: amplitude=-1, frequency=π, and transition zone size of .6.
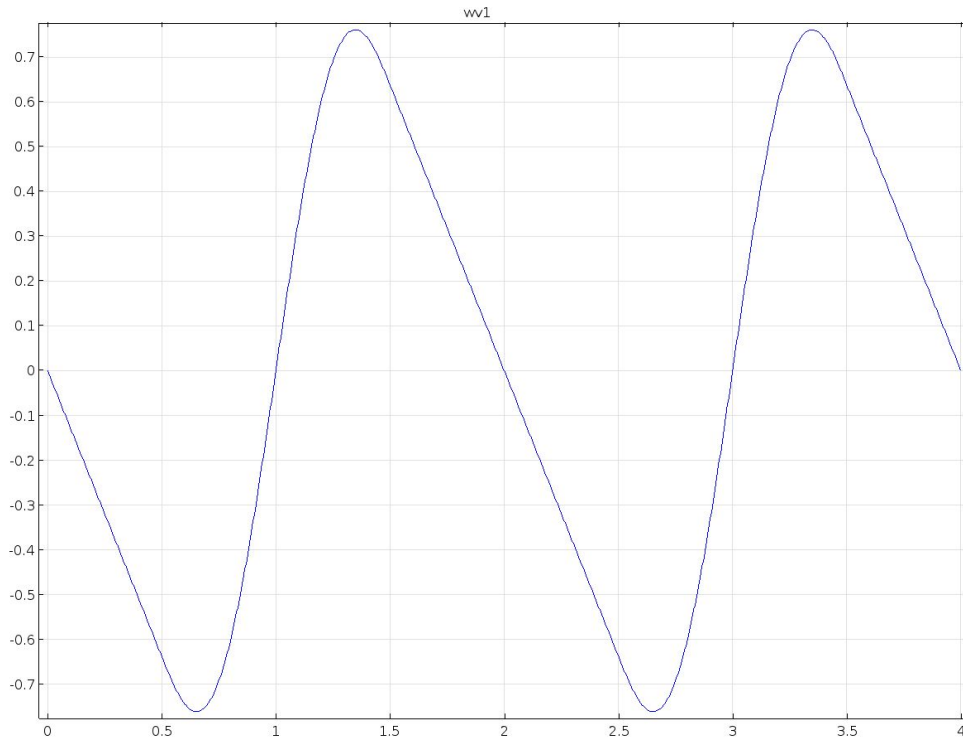
Figure 5

Figure 5 represents the exhale cycle. Through reading we found that during expiration, there is a quick release of air. To better represent that, we used a sawtooth graph with the following settings: amplitude=-1.275, frequency=π, and transition zone size=1.
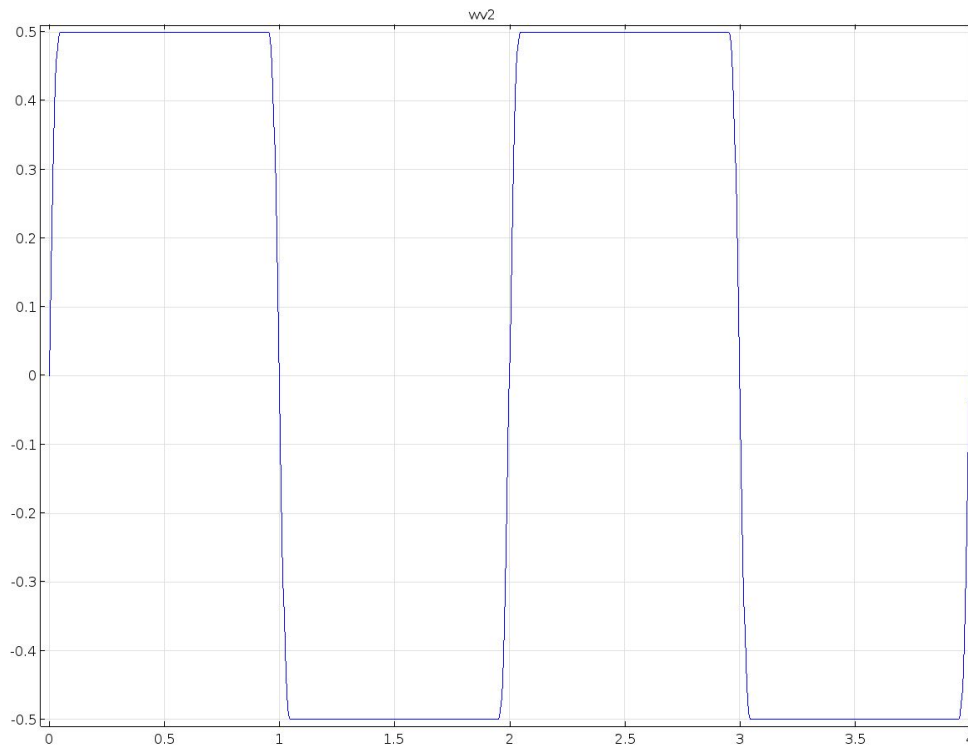
Figure 6

Since we desired 2 different patterns for our inspiration and expiration, it was necessary to formulate a switch between the inhale (**Figure 4**) and the exhale (**Figure 5**). Figure 6 serves as the switching point

$$((.5 + switch) * inhale) + ((.5 - switch) * exhale)$$

Each outlet follows this basic equation and is multiplied by its respective inlet velocity as determined by the following paragraph.

After establishing a tidal volume and breathing pattern, we decided upon flow rates for each segment or lobe applicable to the geometry at hand. Tables 2 and 3 compile the data from Horsfield et al. we used to dictate what percent of the total flow would end up at each outlet. The outlets are labeled counterclockwise from the top left outlet (not inlet). Note how Table 2. Outlet 1 corresponds to Table 3. Outlet 1 + 2 + 3, etc.

$= 0.5L = 0.0005 \; m^3$

$Q = 0.0005 \; m^3 / 2 \; s = 0.00025 \; m^3/s$ (2 seconds corresponds to 15 breaths per minute)

$Q_i = \;_i * \frac{\pi}{4} * d_i^2$

	Diameter (m)	Volume Flow Percentage	Velocity (m/s)
Outlet 1	.0094	20	.7204
Outlet 2	.0110	35	.9208
Outlet 3	.0101	20.3	.7708
Outlet 4	.0087	24.7	.8536

Table 2

	Diameter (m)	Volume Flow Percentage	Velocity (m/s)
Outlet 1	.0031	7	2.319
Outlet 2	.0031	3	0.9935
Outlet 3	.0031	10	3.3125
Outlet 4	.0028	9	3.654

Outlet 5	.0028	6.2	2.517
Outlet 6	.0056	19.8	2.030
Outlet 7	.0056	14	1.421
Outlet 8	.0100	6.3	1.191
Outlet 9	.0056	5.9	0.5990
Outlet 10	.0056	18.8	1.858

Table 3

These velocities represent the average velocity needed through a 2 second inhale or exhale. When we multiply the breathing waveform function by these numbers, there are two consequences worth noting. First, the results are well below what we would expect because we are setting V_{max}, not V_{avg}. These numbers were a good starting point and to further refine them we ran transient simulations, integrated $\int Q\, dt$ and found a correction factor to get our model closer to the exact 0.5L tidal volume. Second, we are "inhaling" much more than we are "exhaling." The disparity between V_{max} and V_{avg} of the square, inhale waveform is much less than the large spike of the modified triangle wave of the exhale waveform that puts its V_{max} at over double its V_{avg}. This means that within the breathing waveform equation for each individual outlet, there is an external term multiplying everything by the corresponding velocity above and two internal terms, an inhale correction factor and an exhale correction factor.

Furthermore, in our model from **Figure 3**, we wanted to translate the data given in volumetric flow (reduced to outlet velocity in our models), into pressure differences. We first ran the geometry through a steady state simulation allowing us to observe the pressure difference generated when the trachea/inlet was set to atmospheric pressure. Once the outlet pressure differences were found, a subsequent series of transient simulations were computed using outlet pressures rather than outlet velocities in order to more perfectly replicate the mechanics of inspiration and expiration. The waveform equation thus had, as mentioned in the last paragraph, just a single term before the exhale section and a single term before the inhale section.

However, in the more complicated geometry of **Figure 3**, we were prevented from converging on a solution with our current computational resources and time available to us. Thus, our **Figure 3** model was computed using only outlet velocities, but data on the pressure gradient was recorded.
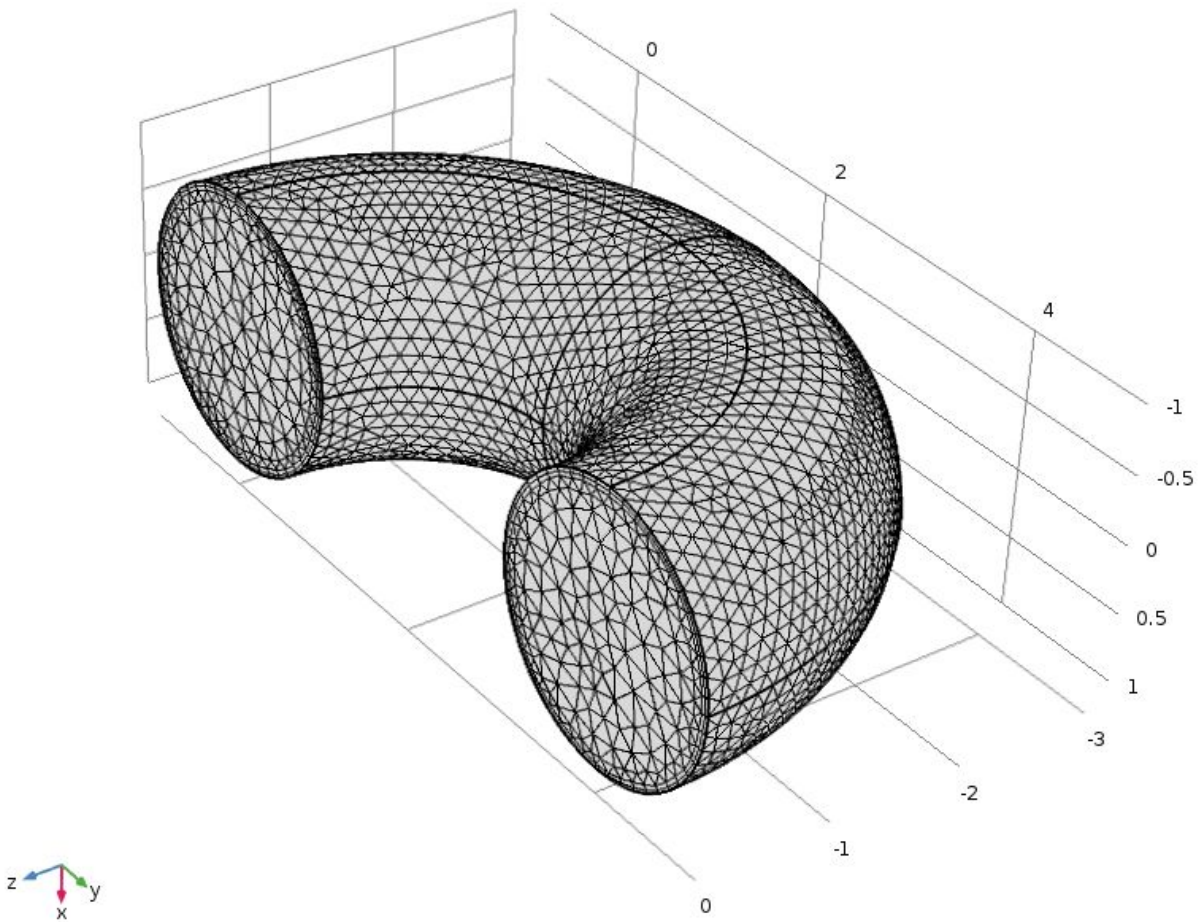
3.2 Hemodynamic System Development
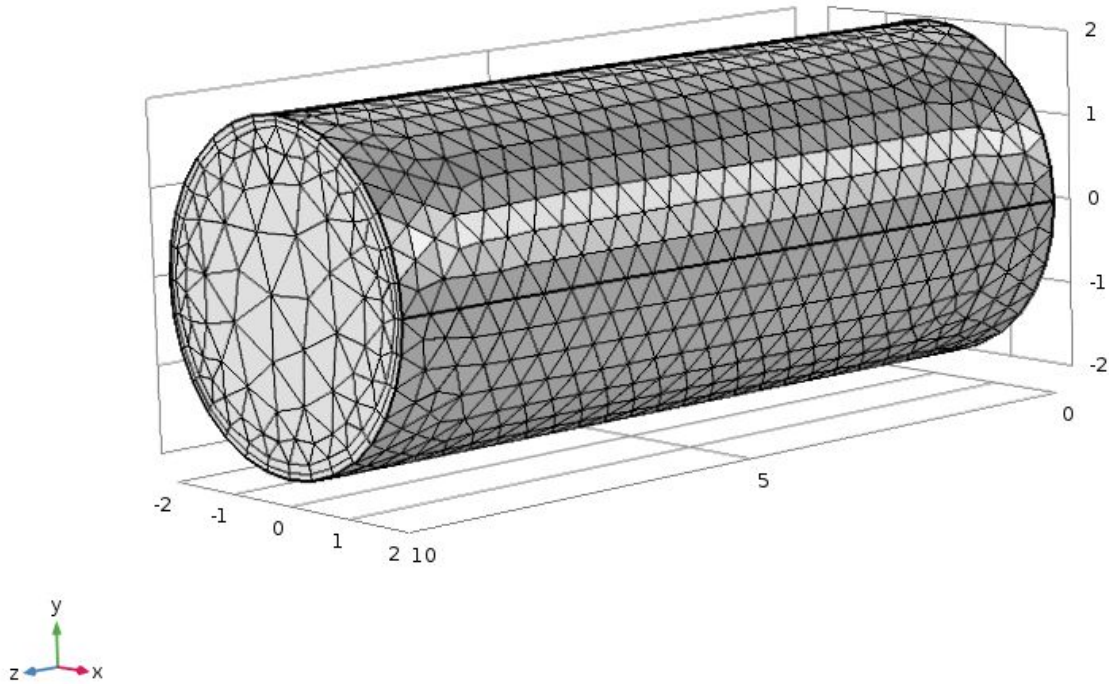
Figure 7

To simulate the pulsatile nature of blood flow, Hemodynamic Simulation 1 was a smooth 3D duct (**Figure 7**) and set the inlet velocity condition according to the following equation (and outlet to atmospheric pressure), using blood values for density and dynamic viscosity, 1060 kg/m³ and 0.005 Pa-s, respectively.

$$V_{inlet}(t) = (Q_{Blood} \div A_{inlet})(1 + sin(\frac{BPM_{Heart}}{60} * 2\pi))$$

Hemodynamic Simulation 2 (**Figure 8**) used the same pulsatile inlet condition, but with a curved geometry that is more representative of what we wanted our final hemodynamic system to look like.

Figure 8

The third and final hemodynamic simulation was a failed attempt at creating a closed loop system, which is elaborated in the discussion section.

3.3 Diffusion and Coupled System Development

The first diffusion simulation concerned moving oxygen from a duct into a spherical representation of the alveoli ("terminal unit"). The physics used are Laminar Flow for CFD and Transport of Concentrated Species (TCS) for oxygen transport (make sure convection is checked under the TCS options), they are coupled together using Comsol's multiphysics flow coupling.

This simulation begins with a steady 0.1 m/s inlet speed (axis is in meters) until the fluid has expanded into the terminal unit. The inlet velocity is then set to 0 and the fluid continues to drift to the right, flowing freely through the rightmost half-circle boundary while the oxygen transport equations have that boundary set as a wall.

Inlet for both fluid flow and oxygen transport:
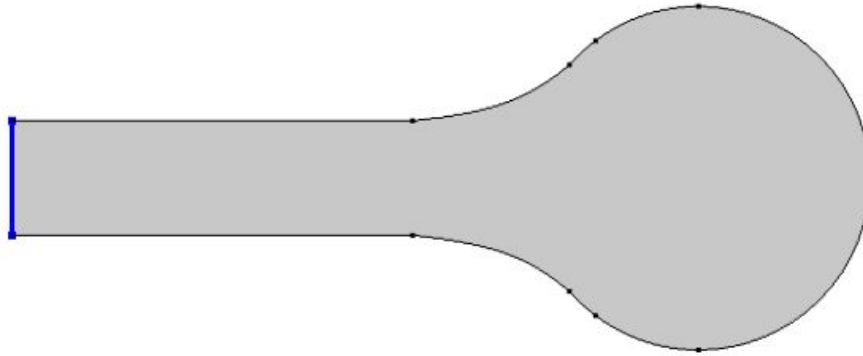
Figure 9

Wall for oxygen transport, outlet for fluid flow:
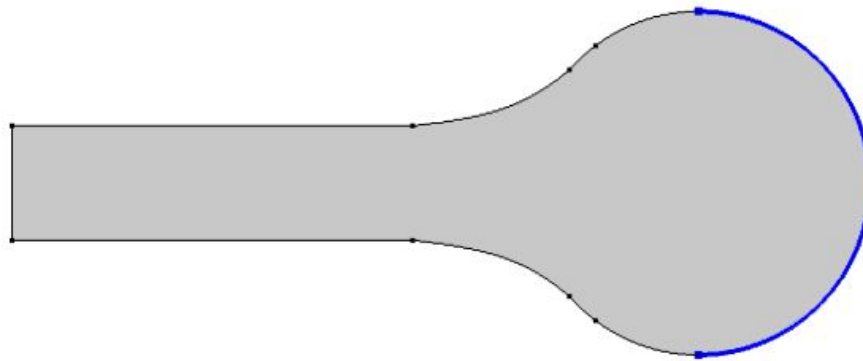
Figure 10

The inlet oxygen concentration is set to 10% by mass, meaning that diffusion alone could only reach the system to a uniform 10% oxygen by mass if there were proper conservation of mass. Since there is flow coupling and the fluid continues through the boundary, the concentration reaches much higher (see color legend for each photo) at the same boundary.

The second diffusion simulation was our first attempt at diffusion oxygen into the blood, coupling the first diffusion simulation with the hemodynamic simulations, as seen in **Figure 11**.
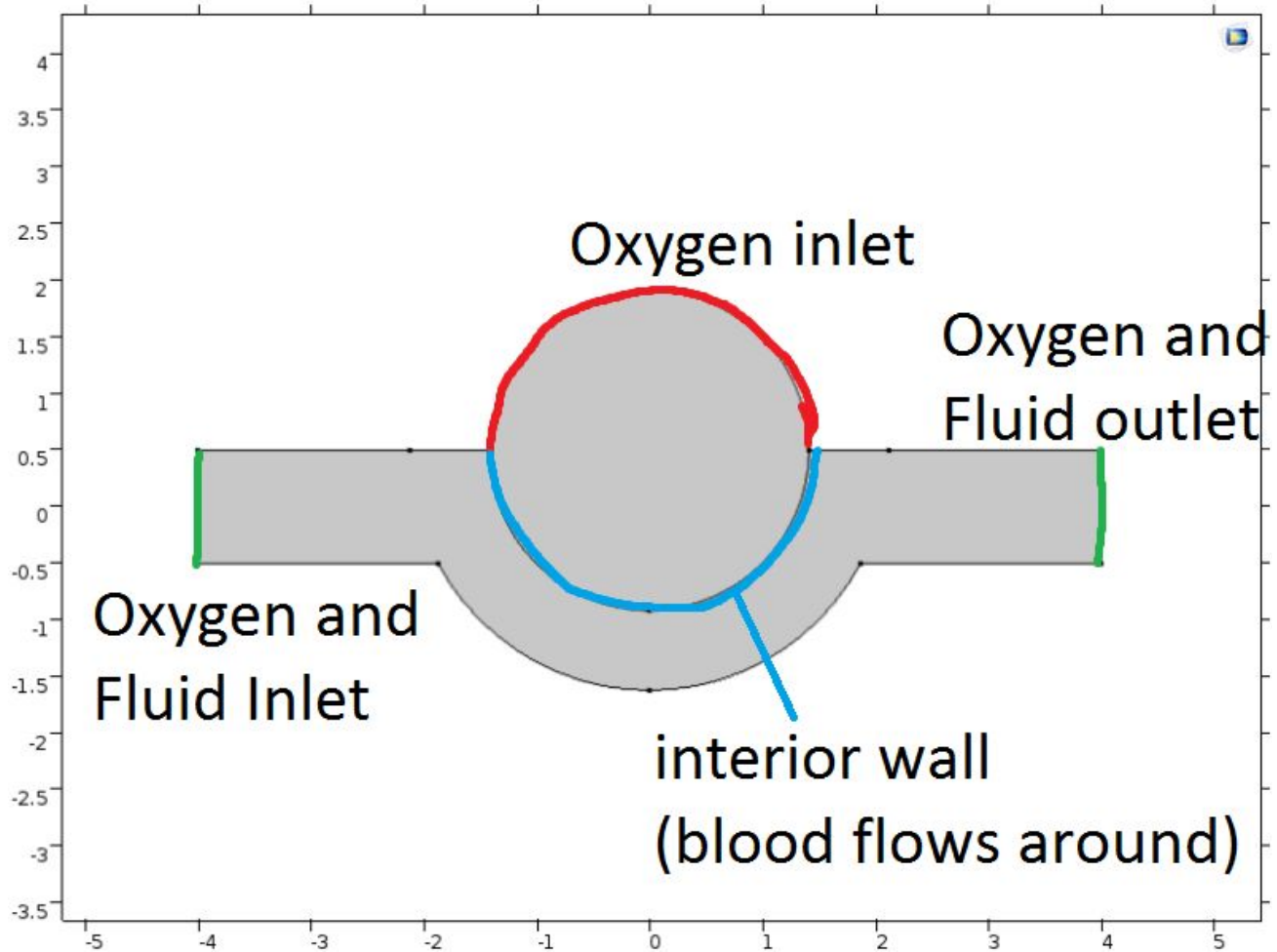
Figure 11

The oxygen concentration at the terminal unit inlet is set to 0.137 mol fraction, mimicking real-world alveolar gas. The hemodynamic inlet was set according to the equation in section 3.2.

4 Results

We were not able to show all the data collected in this paper, but can be found in our supporting Excel documents.

Using at rest breathing conditions specified in the section above, the first series of pulmonary simulations was used for the purpose of computing the pressure difference at the first bifurcation. It is known that the lungs can create a pressure up to ~3 mmHg(400 Pa) found at the terminal units of the lung, the alveolar sacs and pleural lining. In contrast, Figure 1.1 only represents the first generation which we found to have a significantly less pressure.

Pulmonary Simulation 1

Steady State 3D

$V_{avg\ inlet}$= .20571 m/s $P_{avg\ inlet}$=0 Pa
$V_{avg\ outlets}$=.2886 m/s $P_{avg\ outlets}$=-.17657 Pa
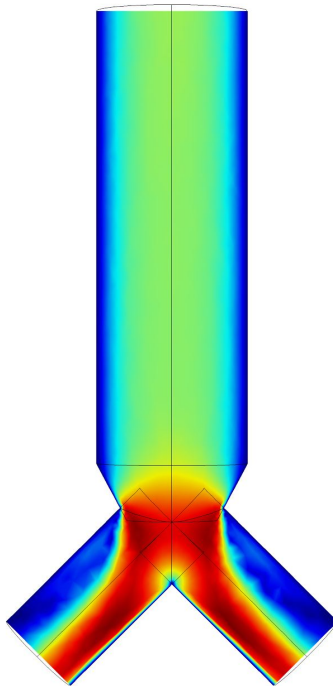
Pulmonary Simulation 2

Transient 3D

This simulation was set to the following initial conditions:

P_{inlet}= wv1(t[1/s]) P_{outlet}= 0 Pa

The dataset will be listed in the appendix. Below is a snapshot of time steps in the animation starting at .1 seconds and ending at 4 seconds.
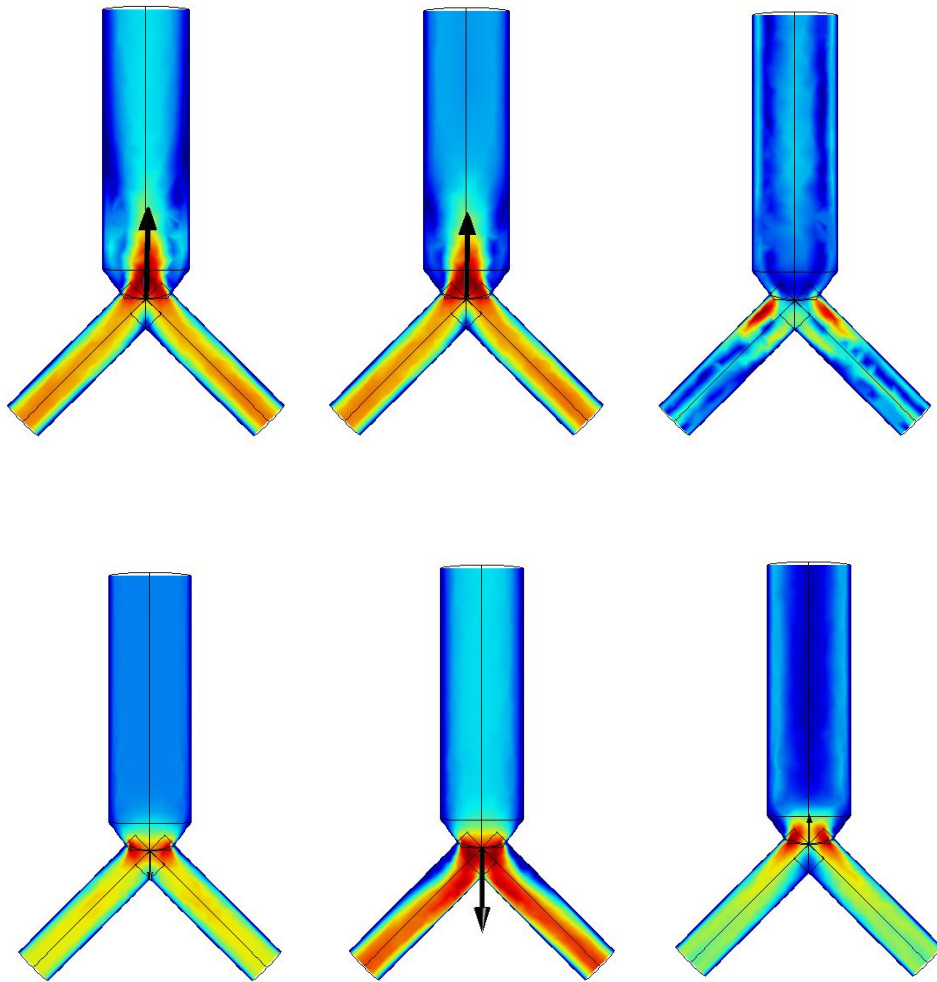
Pulmonary Simulation 3

Steady State 2D

This simulation was set to the following initial conditions:

P_{inlet}= 0 Pa   Outlet1= .1801 m/s   Outlet2=.2302 m/s

Outlet3=.1927 m/s   Outlet4= .2134 m/s

From the above initial conditions the simulation returned the results listed below:

V_{inlet}=.4745 m/s $P_{outlet1}$=.008297 Pa $P_{outlet2}$=.0809 Pa $P_{outlet3}$=.0422 Pa

$P_{outlet4}$=.0121 Pa P_{total}=.1435 Pa

Surface: Velocity magnitude (m/s)
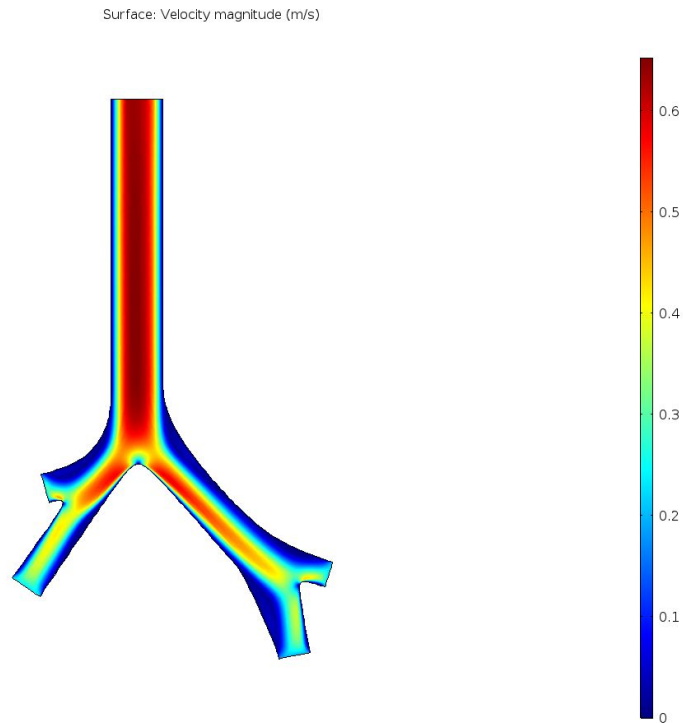
Pulmonary Simulation 4

Transient 2D 2nd Bifurcation

Each outlet was set to its respective speed using the data from Table 3 and our base equation. The dataset for this simulation is listed in the appendix. Below is a snapshot of time steps in the animation starting at .1 seconds and ending at 4 seconds.
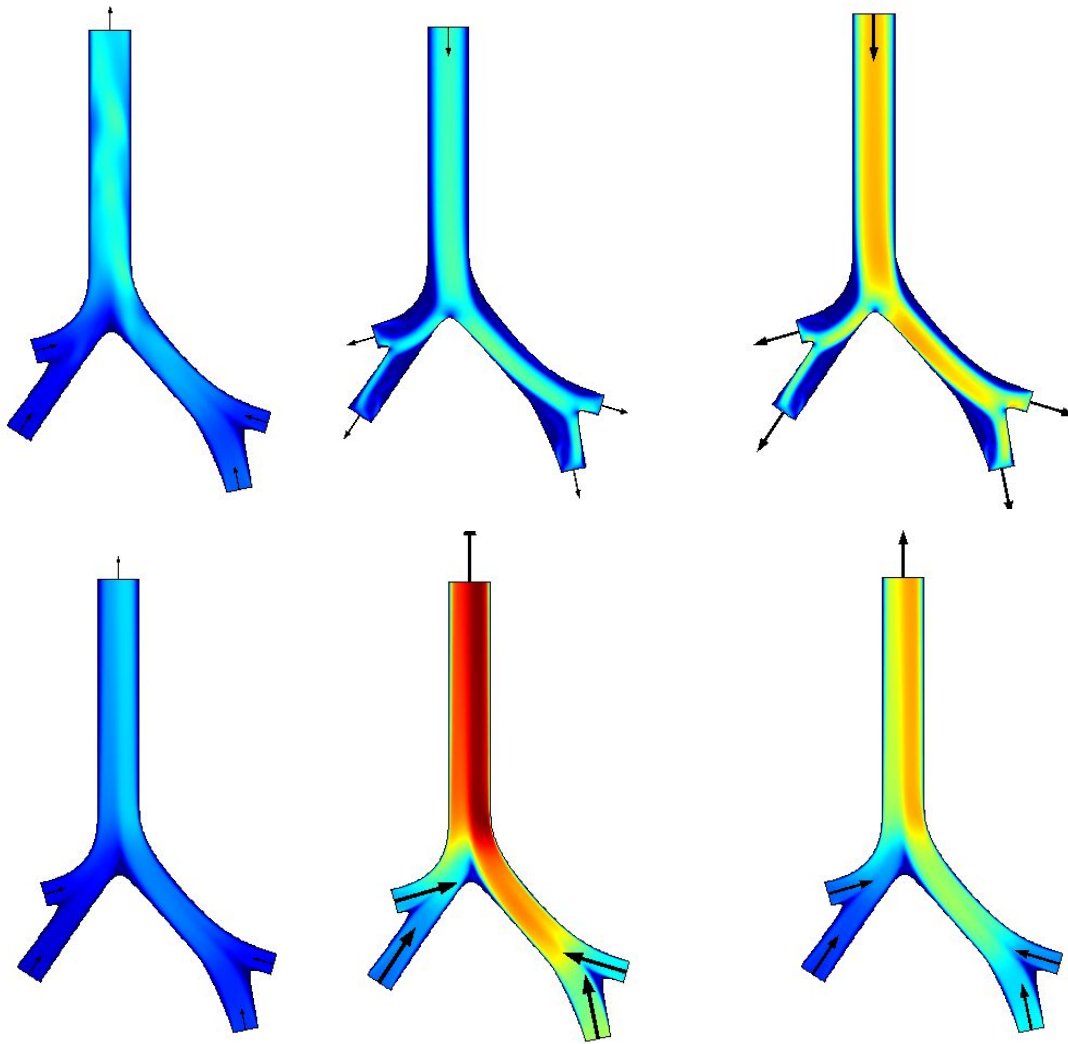
## Pulmonary Simulation 5

Transient 2D 3rd Generation

Each outlet was set to its respective speed using the data from Table 3 and our base equation. The dataset for this simulation is listed in the appendix. Below is a snapshot of time steps in the animation starting at .1 seconds and ending at 4 seconds.
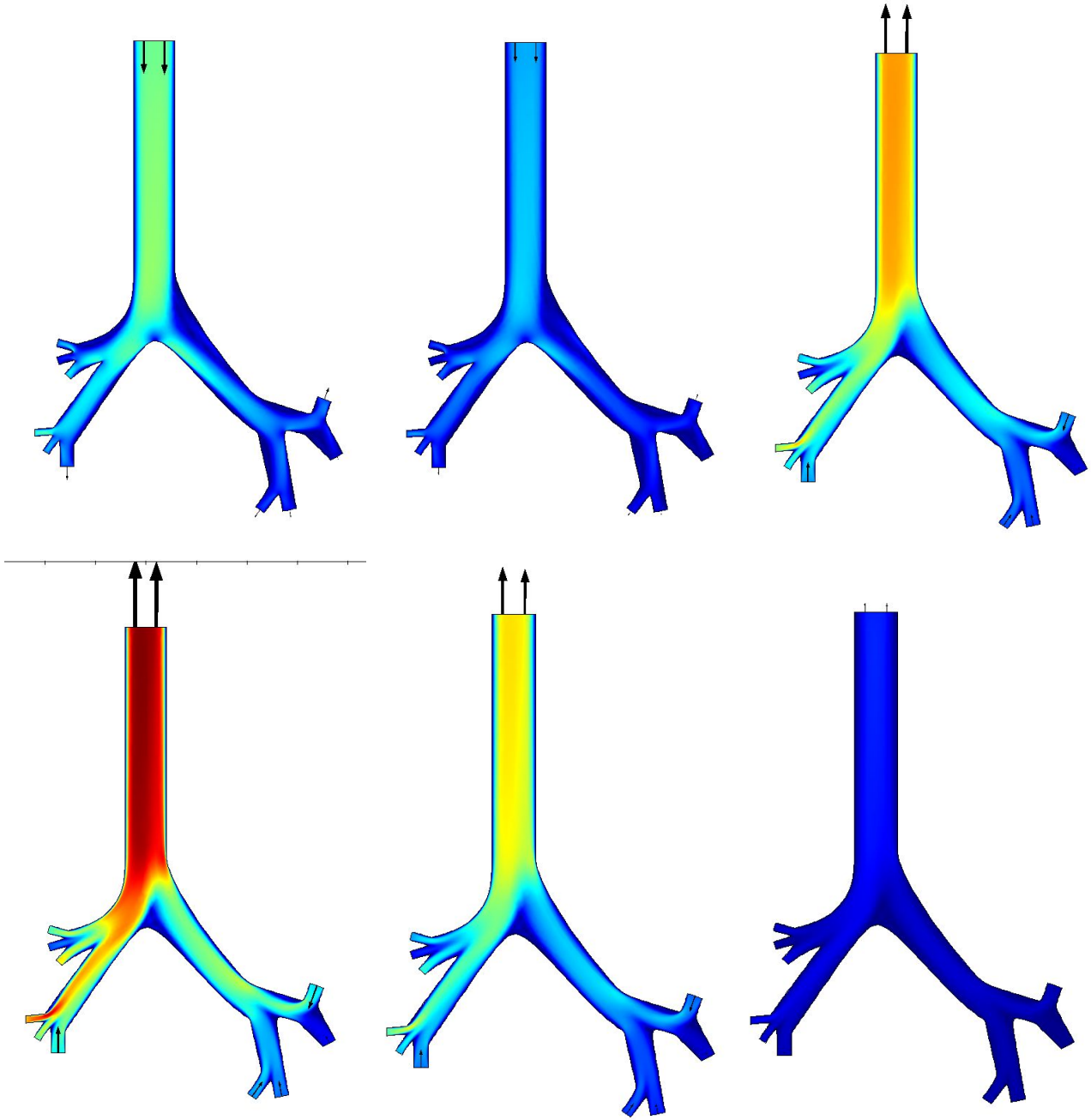
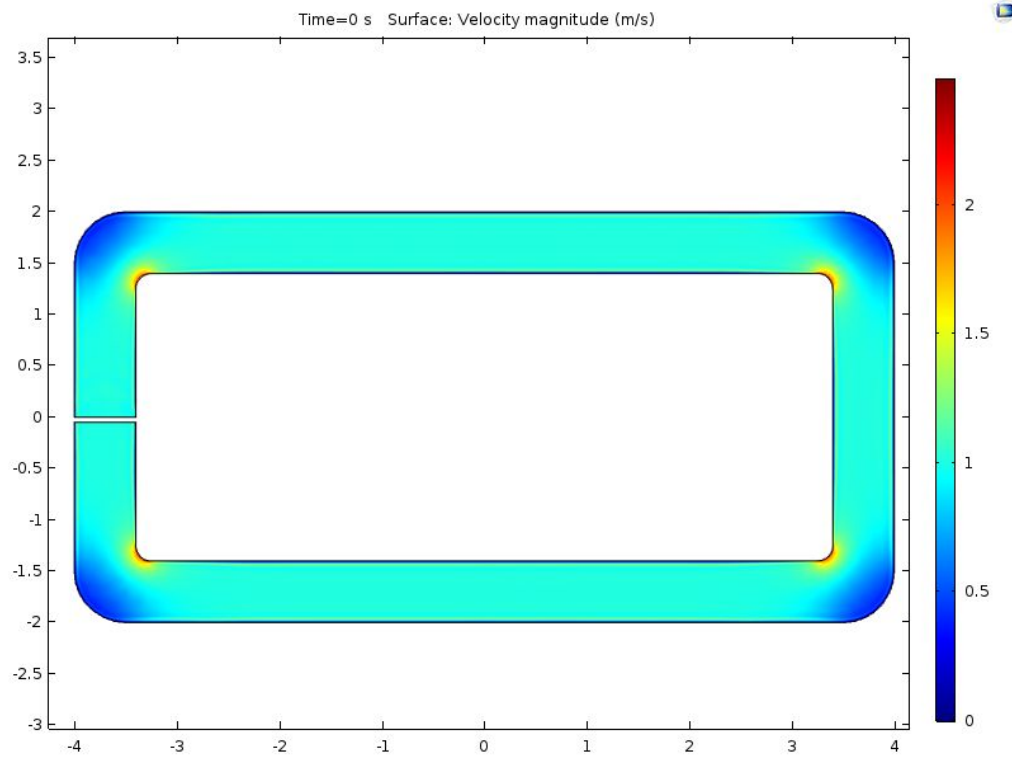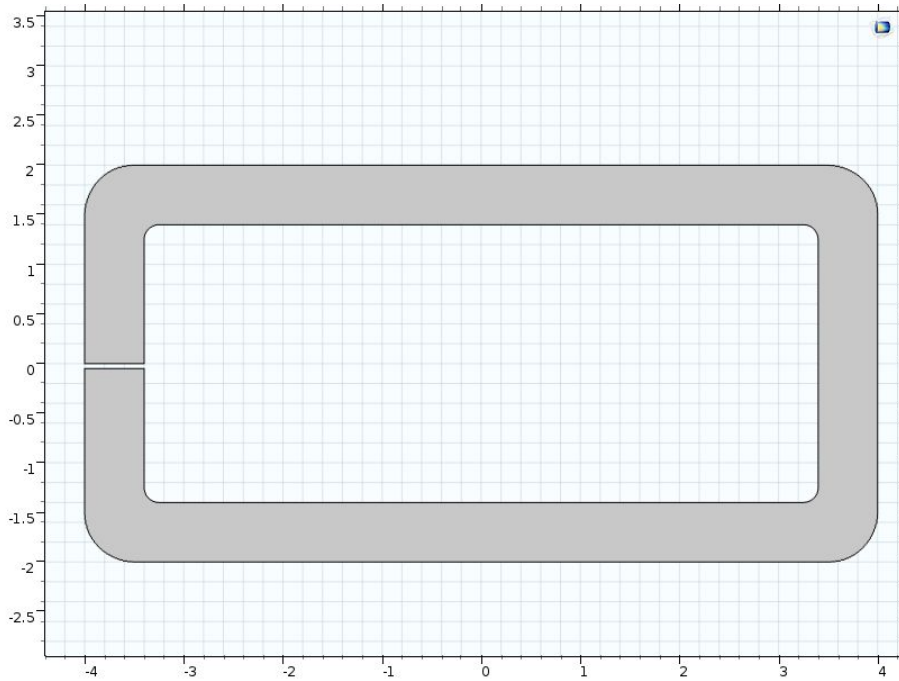Hemodynamic Simulation 1

3D pulsatile flow through a duct
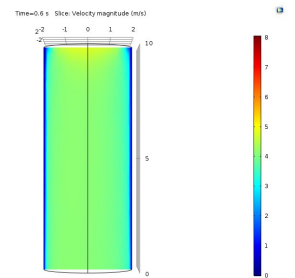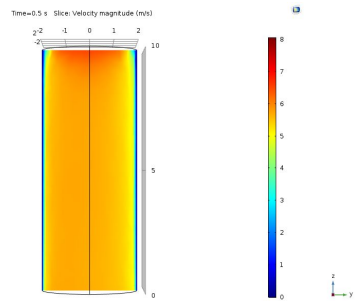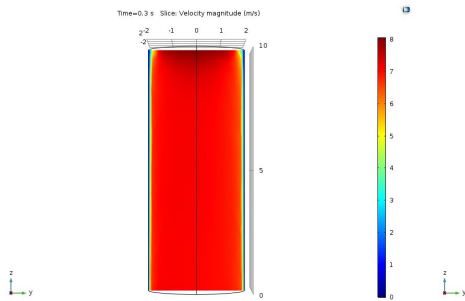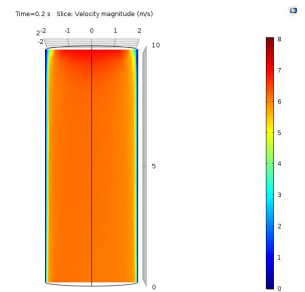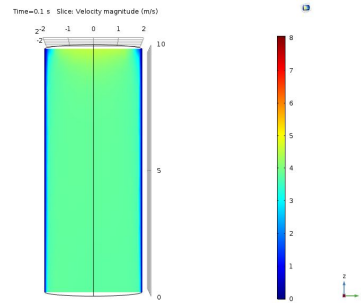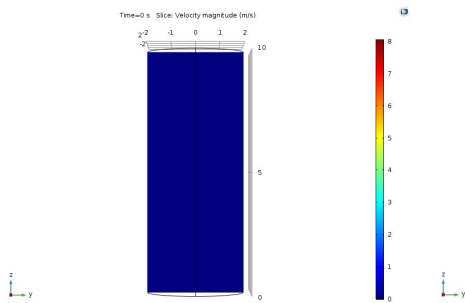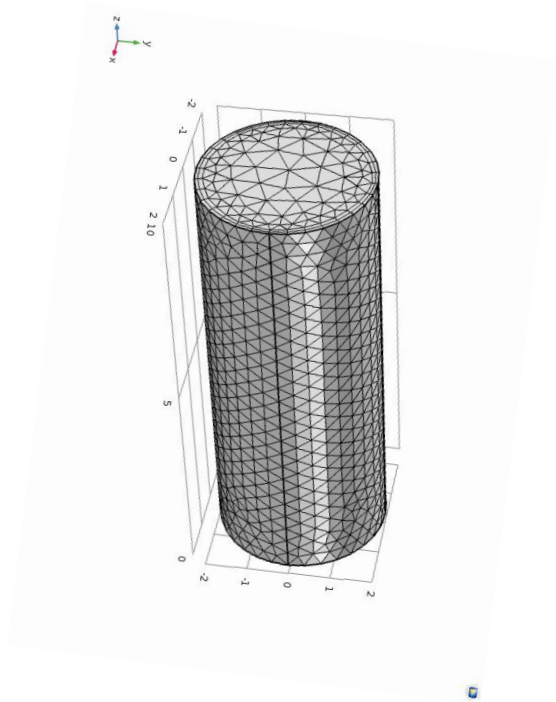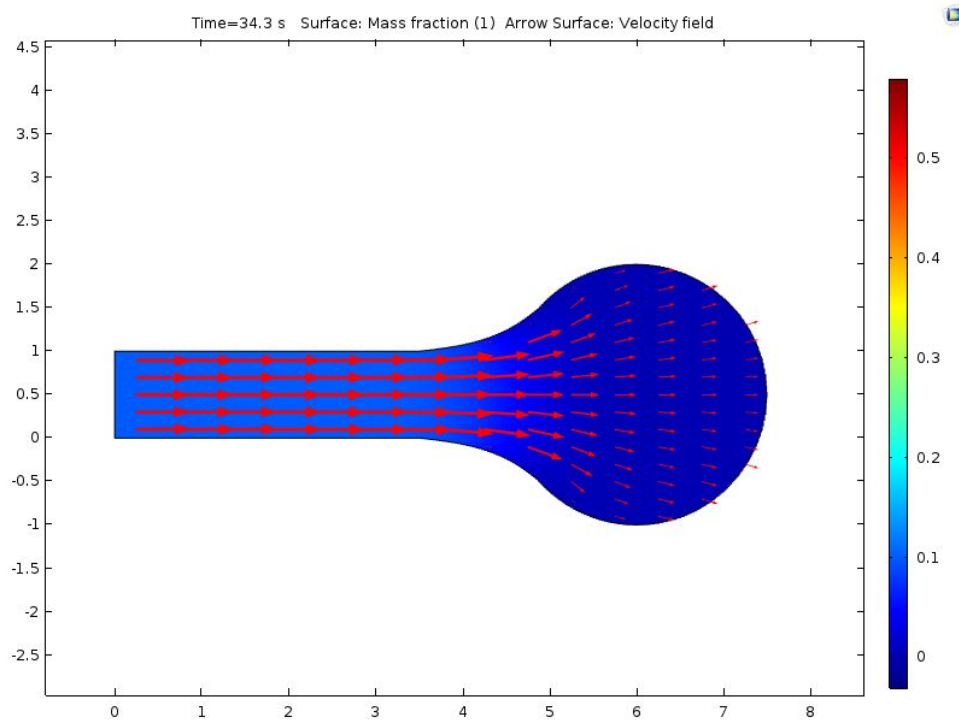
Hemodynamic Simulation 2

3D pulsatile flow through a curved duct
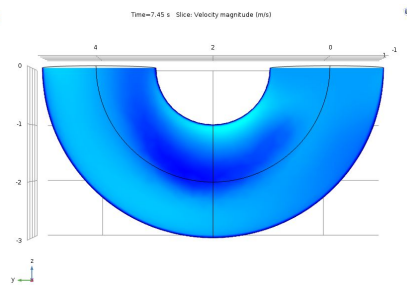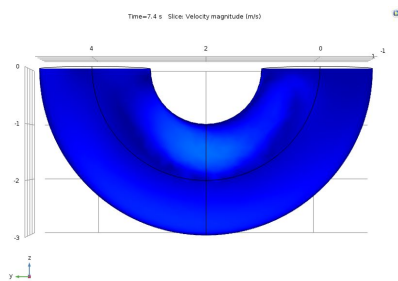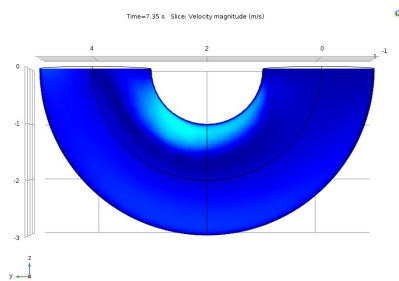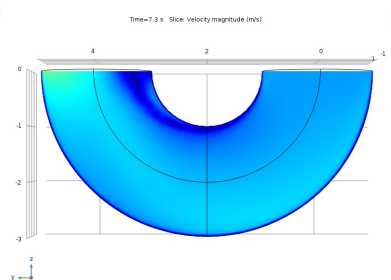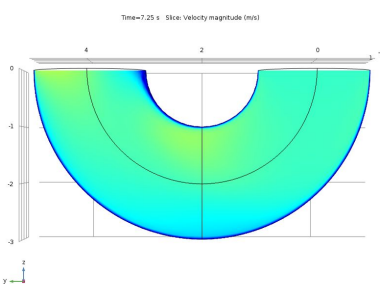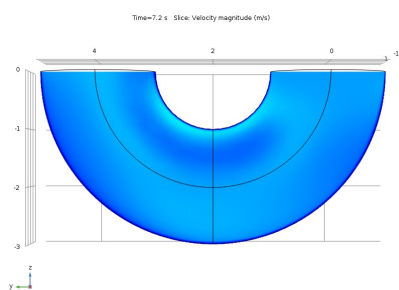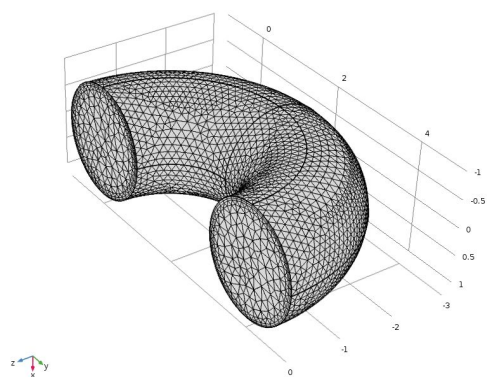
Hemodynamic Simulation 3

Exploring the possibility of a "closed loop" system in Comsol

Time=0 s   Surface: Velocity magnitude (m/s)

Diffusion Simulation 1

Unlike previous photos, the heatmap now represents oxygen concentration (by mass) and the red arrows represent velocity vectors.

Time=6 s   Surface: Mass fraction (1)   Arrow Surface: Velocity field

Time=34.3 s   Surface: Mass fraction (1)   Arrow Surface: Velocity field
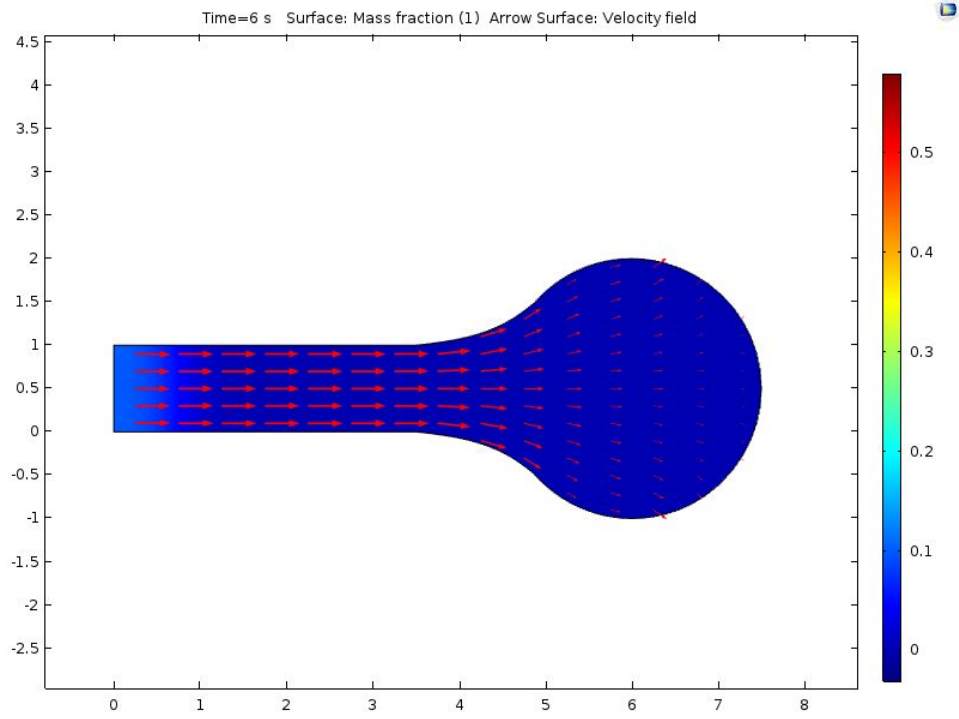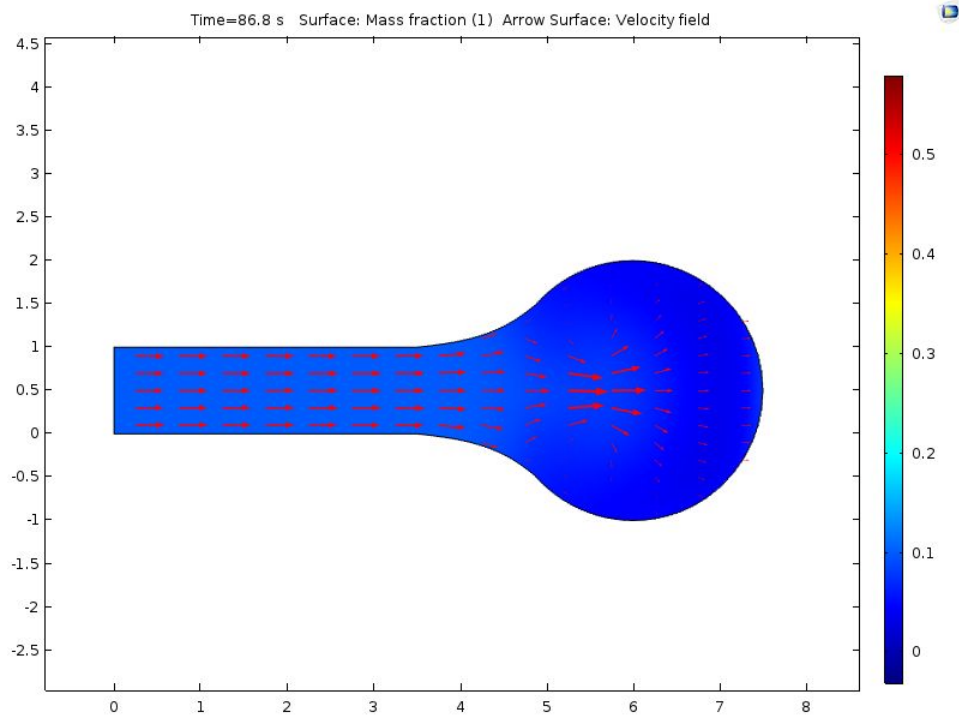
Below: Oxygen begins to be pushed against the wall and concentration skyrockets

Time=107 s   Surface: Mass fraction (1)   Arrow Surface: Velocity field

Time=141.4 s   Surface: Mass fraction (1)   Arrow Surface: Velocity field

Diffusion Simulation 2

Time=0 s   Surface: Mass fraction (1)

Time=0.1 s   Surface: Mass fraction (1)

Time=0.2 s   Surface: Mass fraction (1)

Time=0.3 s   Surface: Mass fraction (1)

Time=0.6 s   Surface: Mass fraction (1)

Time=1.2 s   Surface: Mass fraction (1)

Time=1.4 s   Surface: Mass fraction (1)
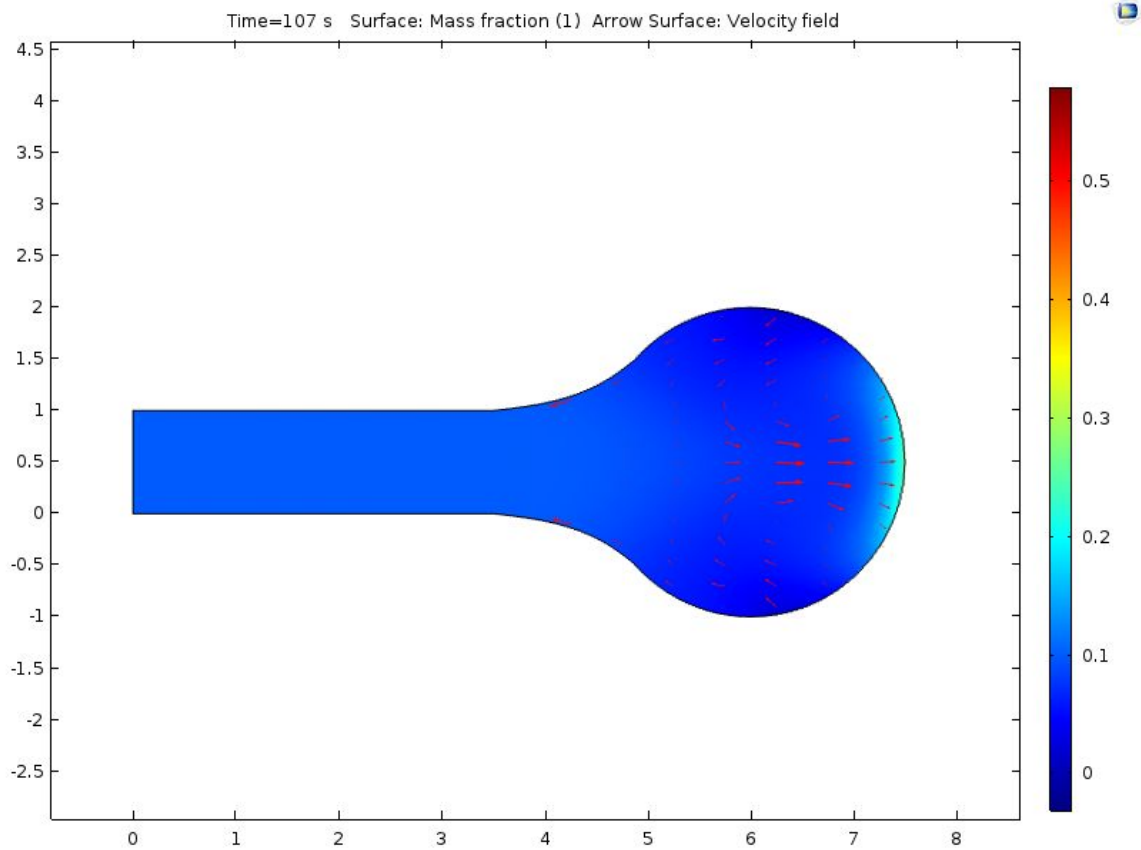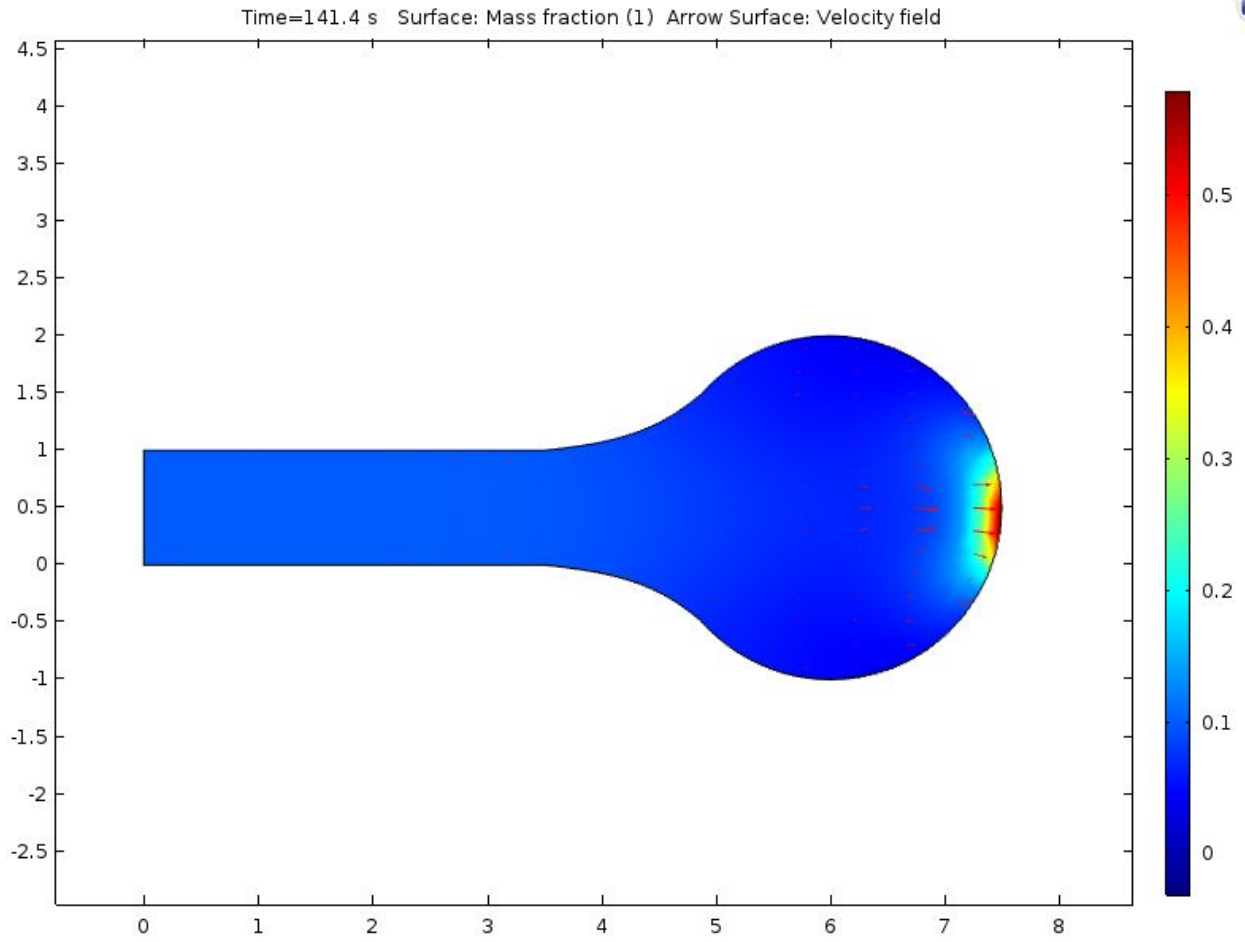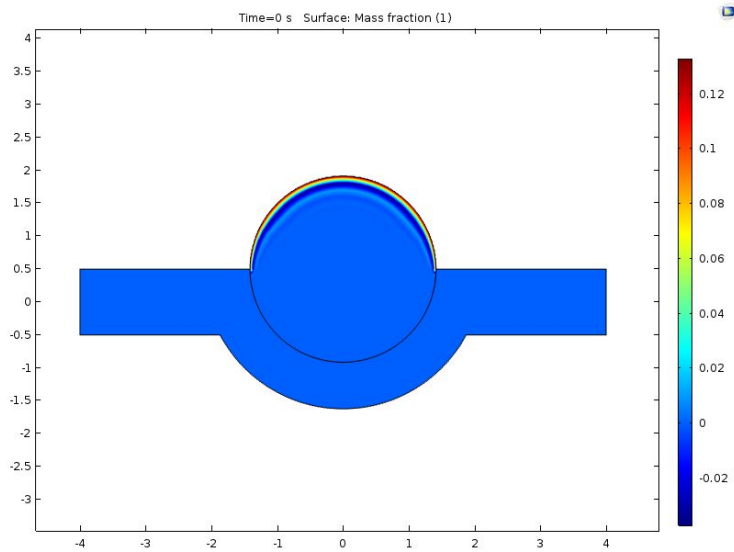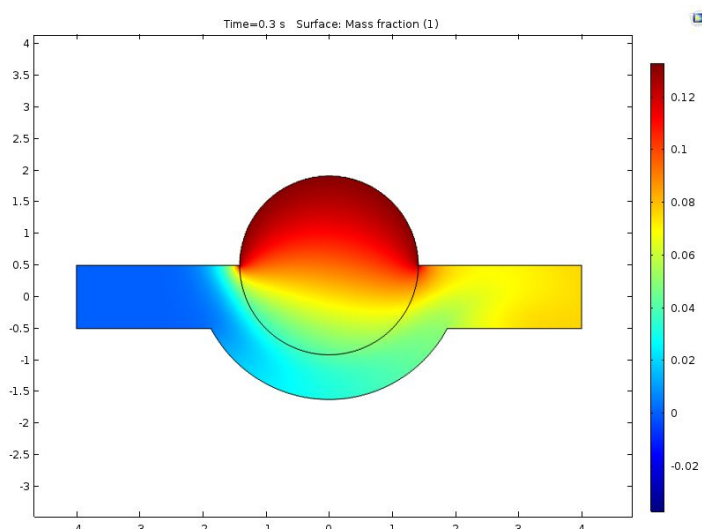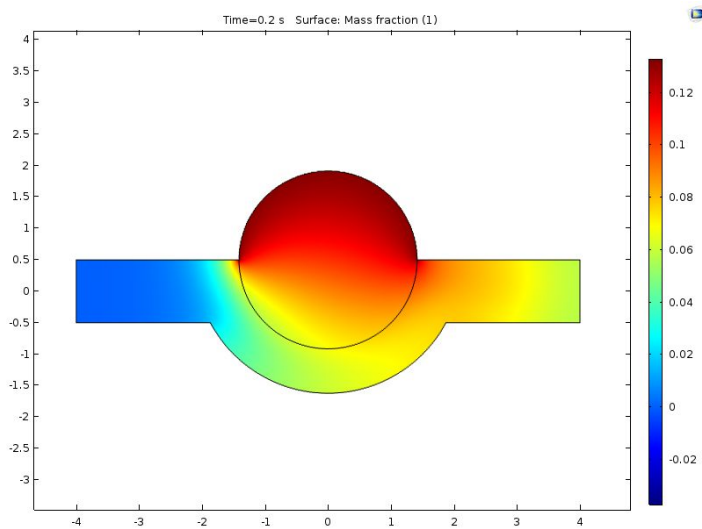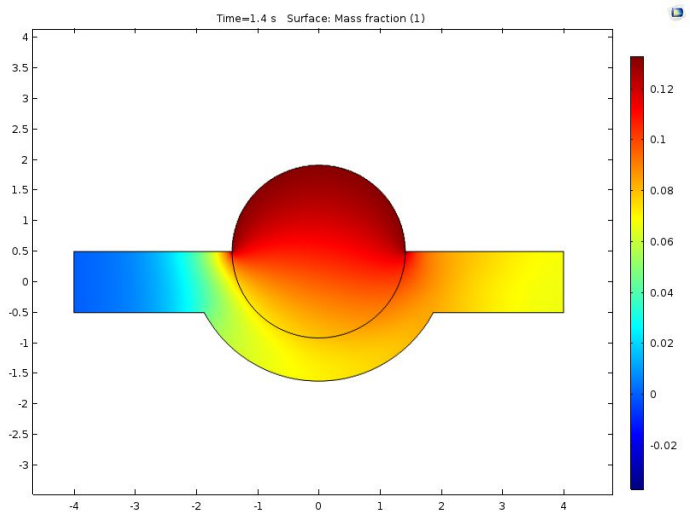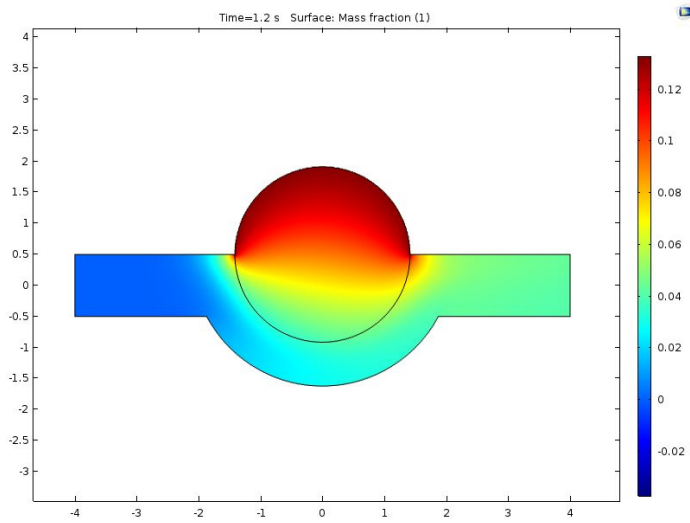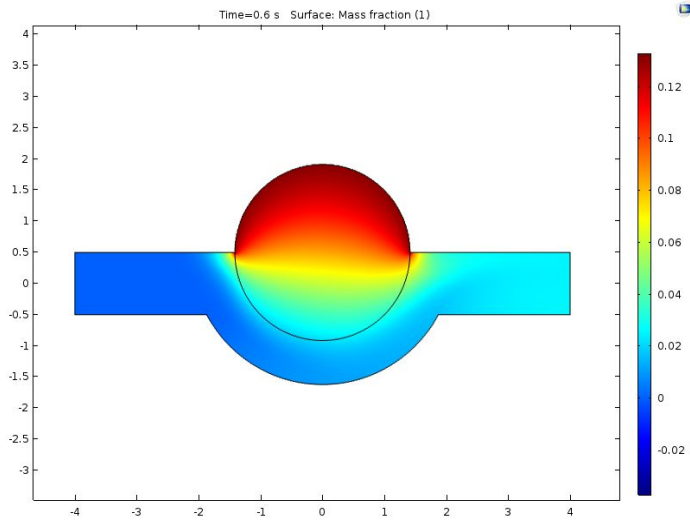
The following data was taken from the the far left and far right inlet/outlet and contains information about the mass flux entering and leaving the system via the blood.

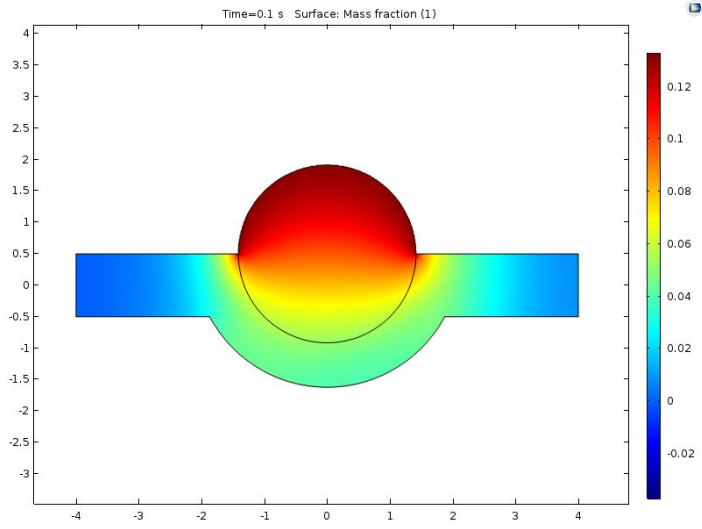|	Value	Unit	
Parameter Length	0.25*pi*diameter	m	
Inlet			
Average Mass Flux	2.91935234E-05	kg/m-s	
Diameter	0.01	m	
Parameterized Mass Flux	2.29285397E-07	kg/s	
Outlet			
Average Mass Flux	0.0030147309	kg/m-s	
Diameter	0.01	m	
Parameterized Mass Flux	2.36776414E-05	kg/s	
Target Inlet Mass Flux	1.61E-05	kg/s	
off by factor of	70.21816585		
Target Outlet Mass Flux	2.14E-05	kg/s	
off by factor of	0.903806239		

Coupled Cardiopulmonary Simulation 1

Our final simulation implements the interface between our pulmonary and blood oxygen diffusion models. There are many current issues with the model as described in the discussion section.
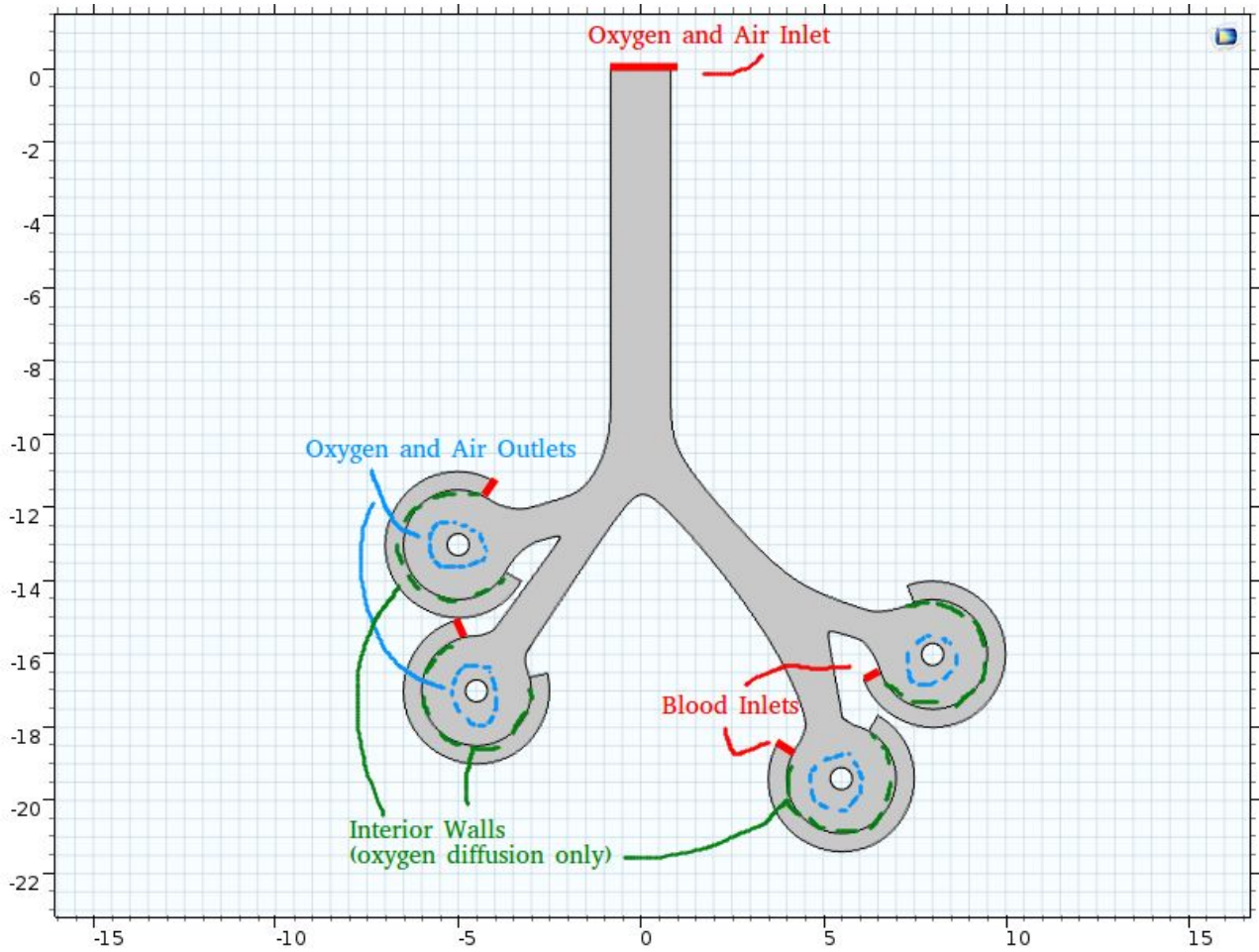
The following photos are from a transient simulation of a continuous inhale (i.e. the inlet speed is a static 1m/s).

Here is the velocity heatmap:

Time=2 s   Surface: Velocity magnitude (m/s)
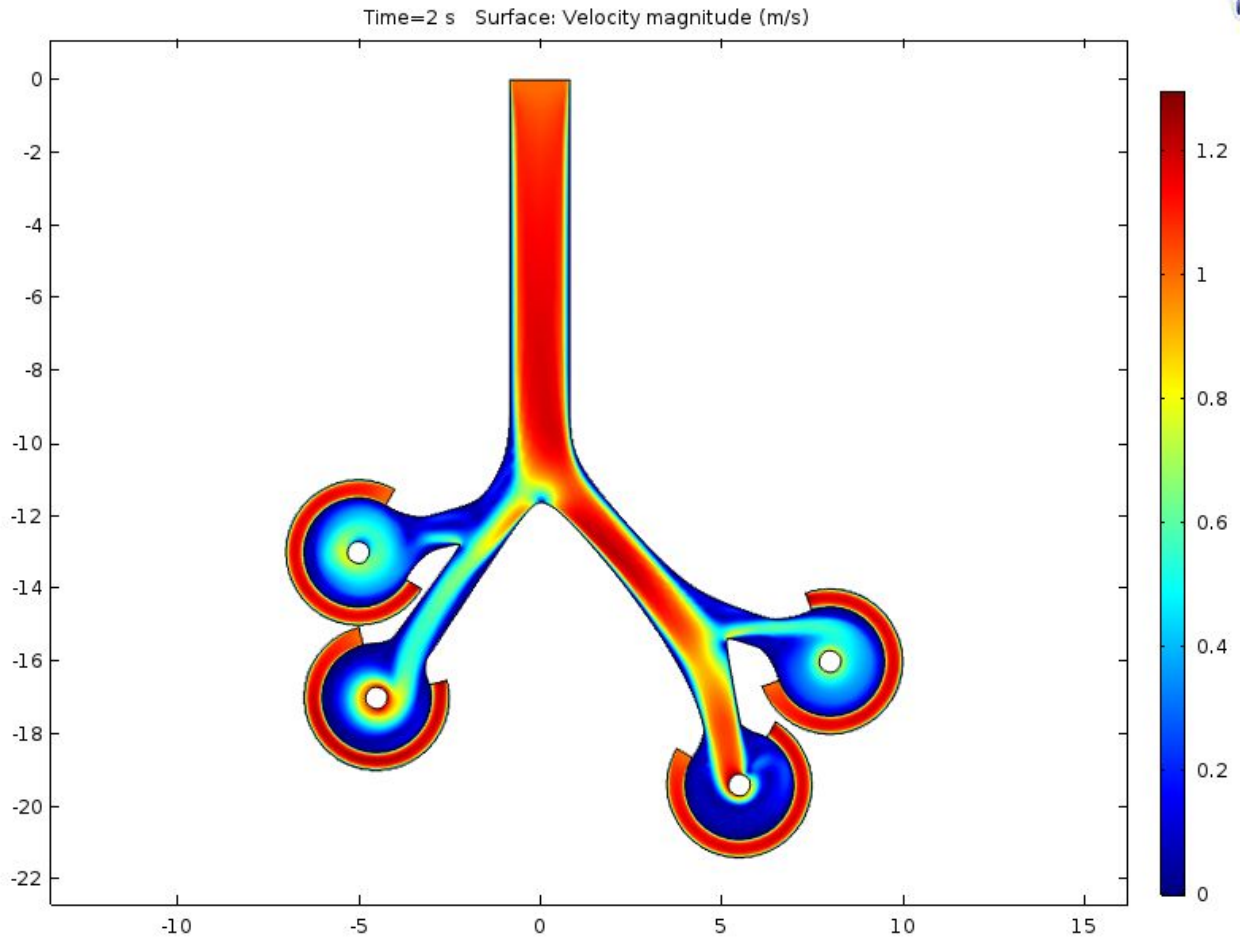
These photos show the oxygen concentration with an initial concentration of 10% by mass for all domains. The arrows represent fluid velocity vectors.

Time=0 s   Surface: Mass fraction (1)   Arrow Surface: Velocity field

Time=0.3 s   Surface: Mass fraction (1)   Arrow Surface: Velocity field

Time=0.5 s   Surface: Mass fraction (1)   Arrow Surface: Velocity field

Time=1 s   Surface: Mass fraction (1) Arrow Surface: Velocity field
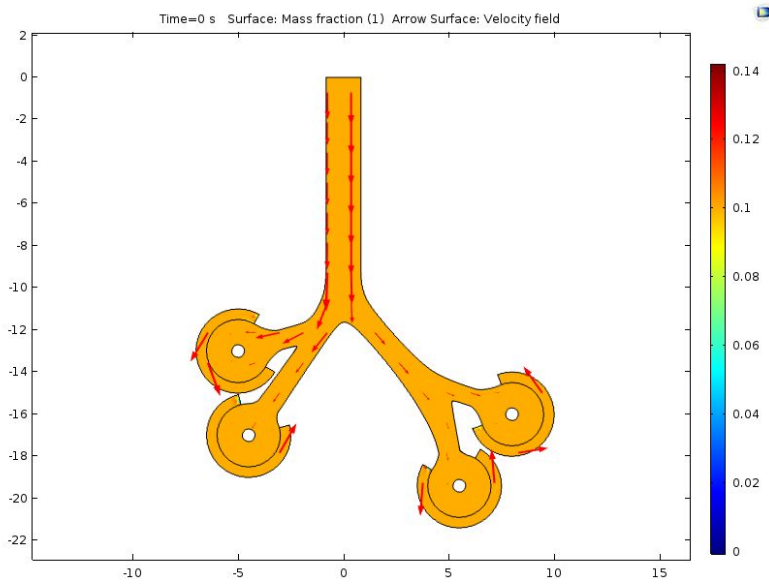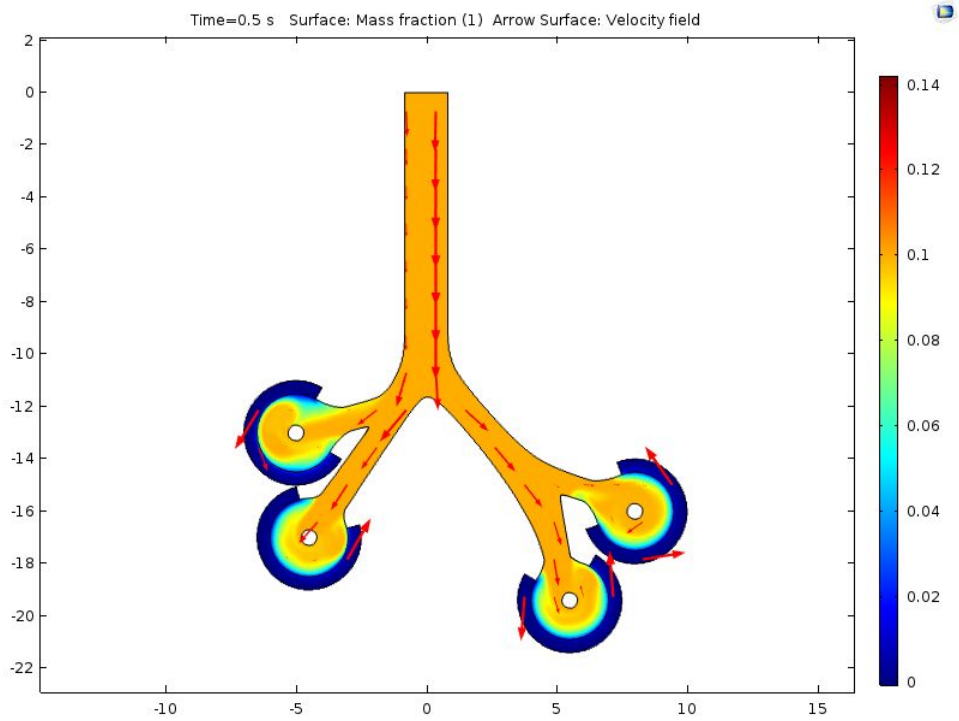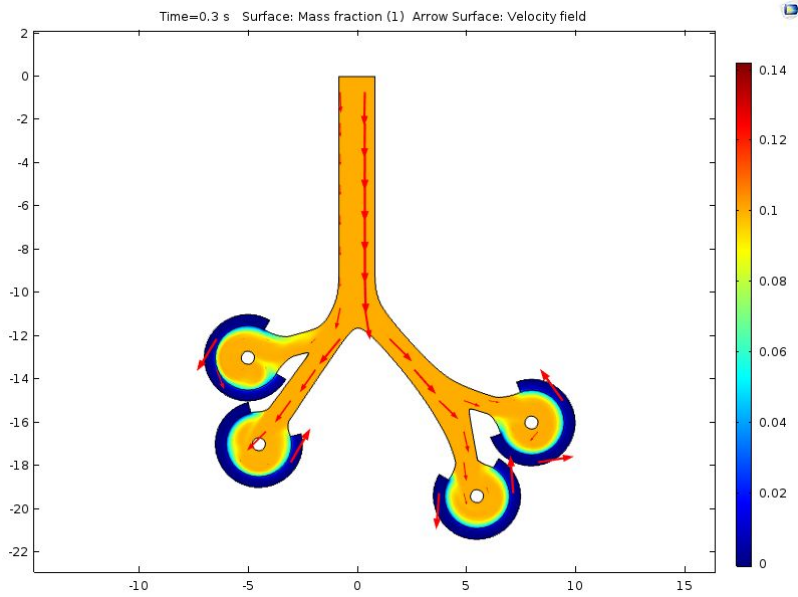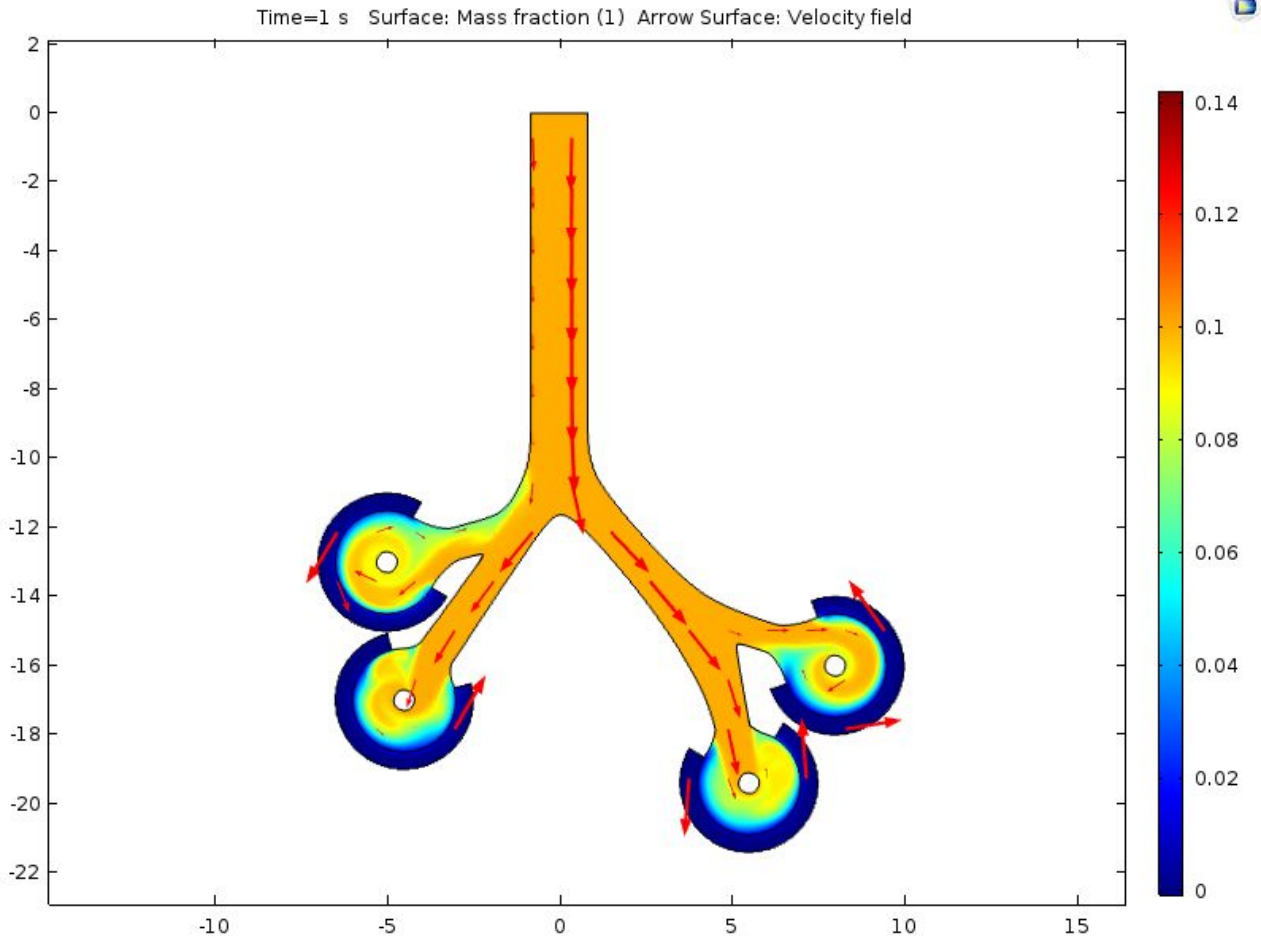
5 Discussion

Pulmonary Simulations 1 and 2

The simulations conducted in 3D were the first footsteps in this project and only served as a reference for future references. In our opinion, the important variables to observe in those simulations are the inlet/outlet flow rates and pressure gradients and those values are listed in our results section.

Pulmonary Simulations 3, 4, and 5

Simulation 3 were the first series of simulations ran with the new geometry shown in **Figure 2**. This was a crucial turning point in the research project, as we felt confident that the data returned would be the most representative of of real world numbers. Simulation 3 results are all compiled in the results section. The pressure difference recorded there informed us of what type of numbers to expect from future simulations.

Simulation 4 was the transient 2D 2nd bifurcation. In order to analyze the data, we decided to take the velocity extracted through Comsol and find the volumetric flow rate(Q) for each time step. After finding Q, we then took the average of Q during inspiration (0-2 seconds) and the average of Q during expiration (2-4 seconds). The volume inhaled and exhaled were calculated, but were not our desired volumes. Furthermore, we found a correction factor for inspiration and expiration with our known desired volume of .00025m^3. Moving forward and replicating this simulation we used those correction factors to replicate the simulation in hopes of achieving closer volume of .00025m^3.

Simulation 5 was the final set of simulations we were able to complete in the duration of this project. Although the method explained above for Simulation 4 was effective for 4 outlets, it would become increasingly less efficient as the number of outlets increased. To analyze the data found in Comsol, we took a similar approach by wanting to compare the volumes inhaled and exhaled, but only observed the inlet boundary of our simulation. Comsol allowed us to take a line integration with the units of m^2/s. After averaging and taking the mean of our integration over our inspiration and expiration time periods, we used our parameterized diameter equation to find Q. With this data, we used the same logic stated above to find correction factors and run the simulation again. We came within a factor of 1 for our desired volume.

Hemodynamic Simulations

Our objective with these simulations were to establish a fluid behavior that would reasonably mimic the general transit of blood through the alveolar capillary mesh. The initial simulation proved that a pulsatile flow was not difficult to converge, followed by a simulation of the curved geometry our final model would boast.

The third simulation of a "closed loop" system answered some questions we had about our bulk continuum. We wanted to relate the outlet of a system to its inlet condition such that after an initial startup period, the system would reach a uniform equilibrium with a linear decrease of oxygen concentration across the loop. Not only was the "closed loop" impossible to implement, but including diffusion out of the blood further complicates our model. We decided against using this method to simulate our bulk continuum.

Diffusion Simulations

Diffusion simulation 1

The curved right wall of this model is set to an outlet for the Navier-Stokes equations, but a wall for the chemical transport equations. We do this because it is easier than simulating the inflation of the terminal unit in Comsol, but we still wanted the oxygen coming into the system. As the results show,

this creates an area of numerical error (the highest O_2 concentration is ~50% by mass with an inlet value of only 10% by mass) that also greatly increases computational requirements.

However, this method creates marked numerical error at the speeds and length scale we are working with. The simulation was done over 200 seconds with *very* slow inlet velocities and a much larger length scale than our final model (meters rather than centimeters), any increase in velocity or decrease in length scale will see the numerical error of the concentration at the wall increase to >100% by mass. In the coupled system, we have solved this problem by creating a "hole" in the center of the terminal unit that acts as an outlet for both fluid and transport equations.

Diffusion simulation 2
This is how we imagined our terminal units to be coupled with our hemodynamic simulations, representative of the alveolar capillary mesh surrounding an alveolar sac. We are not yet coupling the terminal unit to the pulmonary simulations, we left it as a static fluid by which oxygen moves using diffusion only.

During the low-velocity periods of the pulsing flow, the oxygen concentration increases in the curved section of the "blood vessel." The flow then pushes that oxygen out of the system before slowing down to absorb more oxygen.

Coupled System

This coupled system was simulated as a continuous inhale using Comsol's transient solver, this was done because the inclusion of oxygen transport complicates the boundary conditions of the inlet at the trachea and the outlets at the terminal units. We cannot have oxygen both enter and leave from these outlets without creating the numerical error problem mentioned in Diffusion Simulation 1. Yes, the holes in the terminal units create a workable model for a single inhale or exhale, but a time-dependent boundary condition or multi-step solver is required complete a full breath cycle.

6 Summary and Conclusion

Although in today's medical application, 3D models are more favored than 2D models for the purpose physical illustration and easier translation of data, that was not the focus of our project. Our project served as the baseline to have any type of model simulate representative numbers of the pulmonary system and oxygen transport. We were not focused on complex happenings at every bifurcation or endpoints, but more so on the bulk properties expressed through our data. We were

able to achieve a geometry down to the 3rd generation and the methodology we have laid out will give others an easier transition into this project.

       In moving forward with this project, we feel confident in the accuracy of our data to start test simulations of different scenarios. As we model a variety of scenarios, this project will have great use for many, as it will be editable to specific conditions while remaining representative. Also, our formula for creating our geometries are clear enough to create as many generations as wanted with the only limitation of known specifications that far into the tracheobronchial tree. The research we have done and the model we have created will go far in establishing a framework for future projects.

7 Acknowledgements

9 Bibliography

Des Jardins, Terry. *Cardiopulmonary Anatomy and Physiology.* 2002

Hlastala, Michael P., and Albert J. Berger. *Physiology of respiration*. Oxford: Oxford U Press, 2001. Print.

K Horsfield, G Dart, D E Olson, G F Filley, G Cumming. "Models of the human bronchial tree." *Journal of Applied Physiology*, 31(2), 1971, 207-217.

Kim, Chong S. and Fisher, Donald M.. "Deposition Characteristics of Aerosol Particles in Sequentially Bifurcating Airway Models." *Aerosol Science and Technology*, 31(1), 1999, 198-220.

Kevin R. Minard, Andrew P. Kuprat, Senthil Kabilan, Richard E. Jacob, Daniel R. Einstein, James P. Carson, Richard A. Corley. "Phase-contrast MRI and CFD modeling of apparent He gas flow in rat pulmonary airways." *Journal of Magnetic Resonance*, 221(1), 2012, 129-138.

Pennati, Giancarlo et al. "Computational Fluid Dynamics Models and Congenital Heart Diseases." *Frontiers in Pediatrics* 1 (2013): 4. *PMC*. Web. 12 June 2017.

Proetz Aw. "Air currents in the upper respiratory tract and their clinical importance." Ann Otol Rhinol Laryngol, 60(2), 1951, 439-67.

Weidong Mi, Changsheng Zhang, Hong Wang, Jiangbei Cao, Changtian Li, Li Yang, Fang Guo, Xianwang Wang, and Tie Yang. "Measurement and Analysis of the Tracheobronchial Tree in Chinese Population Using Computed Tomography." *PLoS One*, 10, 4, 2015, e0123177.

Longest P. Worth, Tian Geng, Khajeh-Hosseini-Dalasm Navvab, and Hindle Michael. "Validating Whole-Airway CFD Predictions of DPI Aerosol Deposition at Multiple Flow Rates." Journal of Aerosol Medicine and Pulmonary Drug Delivery. December 2016, 29(6): 461-481.

Wu, Zhongjun J. and Taskin, M. Ertan and Zhang, Tao and Fraser, Katharine H. and Griffith, Bartley P. "Computational Model-Based Design of a Wearable Artificial Pump-Lung for Cardiopulmonary/Respiratory Support." *Artificial Organs*, 36(4), 2012, 387-399.

Zhao K, Malhortra P, Rosen D, Dalton P, Pribitkin EA. "Computational fluid dynamics as surgical planning tool: a pilot study on middle turbinate resection." *Anat Rec (Hoboken)*, 297(11), 2014, 2187-95.